Synthesis and Molecular Structures of Neutral Nickel Complexes. Catalytic Activity of (Benzamidinato)(acetylacetonato)nickel for the Addition Polymerization of Norbornene, the Oligomerization of Ethylene, and the Dimerization of Propylene

Elza Nelkenbaum, Moshe Kapon, and Moris S. Eisen*

Department of Chemistry and Institute of Catalysis Science and Technology, Technion-Israel Institute of Technology, Haifa, 32000 Israel

Received December 7, 2004

The new neutral nickel complexes $PhC(NSiMe_3)_2Ni(acac)$ (**3**), $PhC(NSiMe_3)_2Ni(acac)$-(TMEDA) (**4**), $[PhC(NSiMe_3)_2]_2Ni_2$ (**5**), $[PhC(NSiMe_3)_2]_2Ni{\cdot}Li_2Br_2(TMEDA)_2$ (**6**), $(TMEDA)_2Ni$ (**7**), *p*-$MePhC(NSiMe_3)_2Ni(acac)$ (**8**), *p*-$MePhC(NSiMe_3)_2Ni(acac)(TMEDA)$ (**9**), [*p*-MePhC-$(NSiMe_3)_2]_2Ni$ (**10**), $NiMe_2Py_2$ (**11**) and [*p*-$MePhC(NSiMe_3)]_2Ni(Py)$ (**14**) have been synthesized and characterized. The solid-state molecular structures of all complexes have been confirmed by low-temperature X-ray diffraction analysis. The methyl complex *p*-$MePhC(NSiMe_3)_2Ni$-(Me)(Py) (**13**) is not stable and rapidly decomposes, forming the complex [*p*-$MePhC(NSiMe_3)]_2$-Ni(Py) (**14**). Complex **3** activated with MAO has been shown to be an efficient catalytic system for the norbornene vinyl-type polymerization. The activity of the catalyst and the molecular weights of the resulting polynorbornenes were found to be dependent on the reaction time, the MAO/precatalyst ratio, and the reaction temperature. In addition, this catalytic system has been found to dimerize propylene to a mixture of hexenes with a high turnover frequency of $\eta = 9040\ h^{-1}$ and oligomerize ethylene to either a mixture of C_4-C_6 or/and C_4-C_{14} products, depending on the temperature and the solvent, extremely rapidly ($\eta = 83\ 500\ h^{-1}$).

Introduction

While most "single-site" catalytic systems are based on early transition metals and utilized extensively for the coordinative polymerization of nonpolar α-olefins, the use of these catalysts for the copolymerization of functionalized monomers has been limited, due to their highly oxophilic nature.[1] During the past decade, olefin polymerization/oligomerization catalysts promoted by nickel complexes have received increasing interest.[2,3] Their reduced oxophilicity and, hence, their enhanced functional groups tolerance makes them very attractive for the incorporation of polar monomers into a linear polyolefin backbone, yielding polymers with unusual microstructures.[4] However, due to polymerization chain termination via a β-hydrogen elimination process, they were successfully applied for the production of dimers or oligomers of ethylene.[5]

One of the first catalytic systems investigated was a neutral nickel−ylide complex containing a P−O chelate ancillary ligation, which was developed by Keim and employed in the Shell higher olefin process (SHOP) for the synthesis of linear oligomers of ethylene in the C_4-C_{20} range.[6] Higher molecular weight polymers were obtained by using modified SHOP systems, which were found to exhibit modest activities under special conditions.[7]

In the middle of the 1990s the Brookhart and Versipol−DuPont groups introduced a new family of highly active Ni(II) and Pd(II) square-planar cationic olefin polymerization catalysts bonded to bulky aryl-substituted α-diimine (N−N) ligands. These catalysts, being activated with methylalumoxane (MAO), produce a wide range of linear to highly branched high-molecular-weight polyethylenes, depending on the structure of the ancillary ligation and the polymerization conditions.[8] More recently, cationic nickel(II) α-diimine complexes have been shown to copolymerize, at high temperatures and low catalytic activities, ethylene and methyl acrylate.[9]

In view of the high sensitivity of the cationic Ni complexes toward polar substrates in comparison to that of the neutral complexes, there has been a renewed effort for the development of neutral (less electrophilic) nickel-based polymerization catalysts, as they are expected to produce functionalized copolymers. With regard to these neutral complexes a series of neutral nickel(II) catalysts bearing bulky ortho-substituted salicylaldimine ligands have been described recently by Grubbs and co-workers. This new class of neutral complexes operates as single-component catalysts for the homopolymerization of ethylene, exhibiting good

(1) (a) Guram, A. S.; Jordan, R. F. In *Comprehensive Organometallic Chemistry*; Lappert, M. F., Ed.; Pergamon: Oxford, U.K., 1996; pp 589−625. (b) Britovsek, G. J. P.; Gibson, V. C.; Wass, D. F. *Angew. Chem., Int. Ed.* **1999**, *38*, 428.

(2) (a) Ittel, S. D.; Johnson, L. K.; Brookhart, M. *Chem. Rev*. **2000**, *100*, 1169 and references therein. (b) Mecking, S. *Coord. Chem. Rev*. **2000**, *203*, 325. (c) Mecking, S. *Angew. Chem., Int. Ed.* **2001**, *40*, 534. (d) Gibson, V. C.; Spitzmesser, S. K. *Chem. Rev*. **2003**, *103*, 283. (e) Rieger, B.; Baugh, L. S.; Kacker, S.; Striegler, S., Eds. *Late Transition Metal Polymerization Catalysis*; Wiley-VCH: Weinheim, Germany, 2003.

10.1021/om0490379 CCC: $30.25
Publication on Web 04/23/2005

functional group tolerance and remaining active in the presence of polar solvents.[10]

Gibson and co-workers have reported on a new nickel catalysts containing bulky anthracenyl-derived (P−O) chelating ligation. These catalysts were found capable of copolymerizing ethylene with methyl methacrylate (MMA), producing a functionalized polyethylene in which the incorporated MMA group appears at the chain ends. In addition, oligomers of propylene with 1-hexene were obtained by the use of these complexes.[11] Brookhart and co-workers have reported on highly active neutral nickel polymerization catalysts that do not require a cocatalyst, which are derived from the 2-anilinotropone[12] and anilinoperinaphthenone [13] ligands, forming five-membered chelate (N−O) rings with the metal. The most remarkable finding with these neutral catalysts is that the microstructure of the produced polyethylenes is similar to that obtained by using α-diimine Ni(II) complexes activated with MAO.

To date, the search for new ligand structures represents a major route to designing novel α-olefin polymerization catalysts. A wide variety of neutral nickel catalysts bearing different ancillary ligands such as pyridinecarboxylate,[14] phosphinosulfonamide,[15] diazene,[16] β-diketiminate,[17] amino-*p*-benzoqinone,[18] (2-pyridyl)benzamide,[19] and 1-azaallyl,[20] has been described. In addition to α-olefins, nickel complexes have been also utilized for the polymerization of bicyclo[2.2.1]-hept-2-ene (norbornene), yielding saturated polymers. Nickel precursors containing the chelating acetylacetonate,[21] 2-(diphenylamino)benzoate,[22] pyrrolimine,[23] salen,[24] Schiff base,[17c] and (salicylideneiminato)[25] ligands comprise some of the systems that have been studied for the homo- and/or copolymerization of norbornene.

Our previous developments in the use of benzamidinate ancillary ligands with early transition metals as active catalysts for the polymerization of α-olefins have encouraged us to investigate the reactivity of the nickel metal toward those ligations. Here we report on the synthesis and structural X-ray diffraction studies on seven new neutral nickel(II) complexes containing the benzamidinate ligand, forming four- and five-membered rings. The *N*,*N*′-bis(trimethylsilyl)benzamidinate and *N*,*N*′-bis(trimethylsilyl)toluimidinate ligands were cho-

(3) (a) Zou, H.; Zhu, F. M.; Wu, Q.; Al, J. Y.; Lin, S. A. *J. Polym. Sci. A: Polym. Chem.* **2005**, *43*, 1325. (b) Wang, X.; Liu, S.; Jin, G.-X. *Organometallics* **2004**, *23*, 6002. (c) Tang, X.; Cui, Y.; Sun, W.-H.; Miao, Z.; Yan, S. *Polym. Int.* **2004**, *53*, 2155. (d) Bluhm, M. E.; Folli, C.; Walter, O.; Döring, M. *J. Mol. Catal. A: Chem.* **2005**, *229*, 177. (e) Du, J.; Li, L.-J.; Li, Y. *Inorg. Chem. Commun.* **2005**, *8*, 246. (f) Chen, Y.; Wu, G.; Bazan, G. C. *Angew. Chem., Int. Ed.* **2005**, *44*, 1108. (g) Speiser, F.; Braunstein, P.; Saussine, L. *Organometallics* **2004**, *23*, 2625. (h) Speiser, F.; Braunstein, P.; Saussine, L. *Dalton* **2004**, 1539. (i) Speiser, F.; Braunstein, P.; Saussine, L.; Welter, R. *Organometallics* **2004**, *23*, 2613. (j) Speiser, F.; Braunstein, P.; Saussine, L.; Welter, R. *Inorg. Chem.* **2004**, *43*, 1649. (k) Speiser, F.; Braunstein, P. *Inorg. Chem.* **2004**, *43*, 4234. (l) Kwon, H. Y.; Lee, S. Y.; Lee, B. Y.; Shin, D. M.; Chung, Y. K. *Dalton* **2004**, 921. (m) Zhang, Q.-X.; Lin, S.-Q.; Wu, Z.-Y.; Wang, H.-H. *Gaodeng Xuexiao Huaxue Xuebao* **2004**, *25*, 2166. (n) Dennett, J. N. L.; Gillon, A. L.; Heslop, K.; Hyett, D. J.; Fleming, J. S.; Lloyd-Jones, C. E.; Orpen, A. G.; Pringle, P. G.; Wass, D. F.; Scutt, J. N.; Weatherhead, R. H. *Organometallics* **2004**, *23*, 6077. (o) Mueller, C.; Ackerman, L. J.; Reek, J. N. H.; Kamer, P. C. J.; van Leeuwen, P. W. N. M. *J. Am. Chem. Soc.* **2004**, *126*, 14960. (p) Gibson, V. C.; Tomov, A. PCT Int. Appl. 2004, 120 pp. (q) Kogut, E.; Zeller, A.; Warren, T. H.; Strassner, T. *J. Am. Chem. Soc.* **2004**, *126*, 11984. (r) Zhang, Q.-X.; Lin, S.-G.; Wu, Z.-Y.; Wang, H.-H. *Chin. J. Polym. Sci.* **2004**, *22*, 313. (s) Heinicke, J.; Koehler, M., Peulecke, N.; Keim, W.; Jones, P. G. *Z. Anorg. Allg. Chem.* **2004**, *630*, 1181. (t) Zhao, W.; Qian, Y.; Huang, J.; Duan, J. *J. Organomet. Chem.* **2004**, *689*, 2614. (u) Suzuki, H.; Matsumura, S.; Satoh, Y.; Sogoh, K.; Yasuda, H. *React. Funct. Polym.* **2004**, *59*, 253. (v) Hulea, V.; Fajula, F. *J. Catal.* **2004**, *225*, 213. (w) Heinicke, J.; Koehler, M.; Peulecke, N.; Keim, W. *J. Catal.* **2004**, *225*, 16. (x) Zhao, B.; Kacker, S.; Canich, J. A. M. PCT Int. Appl. 2004, 58 pp. (y) Heveling, J.; Nicolaides, C.; Christakis, P.; Scurrell, M. S. *Catal. Lett.* **2004**, *95*, 87. (z) Wasserscheid, P.; Hilgers, C.; Keim, W. *J. Mol. Catal. A: Chem.* **2004**, *214*, 83. (aa) Qian, Y.; Zhao, W.; Huang, J. *Inorg. Chem. Commun.* **2004**, *7*, 459. (bb) Albers, I.; Alvarez, E.; Campora, J.; Maya, C. M.; Palma, P.; Sanchez, L. J.; Passaglia, E. *J. Organomet. Chem.* **2004**, *689*, 833. (cc) Tobisch, S. *J. Am. Chem. Soc.* **2004**, *126*, 259. (dd) Myagmarsuren, G.; Yong Jeong, O.; Ihm, S.-K. *Appl. Catal. A* **2004**, *275*, 271. (ee) Suzuki, H.; Matsumura, S.; Satoh, Y.; Sogoh, K.; Yasuda, H. *React. Funct. Polym.* **2004**, 58, 77.

(4) Boffa, L. S.; Novak, B. M. *Chem. Rev.* **2000**, *100*, 1479 and references therein.

(5) (a) Peuckert, M.; Keim, W. *Organometallics* **1983**, *2*, 594. (b) Wilke, G. *Angew. Chem., Int. Ed.* **1988**, *27*, 185. (c) Mitkova, M.; Kurtev, K.; Zlotskii, S. S.; Rakhmankulov, D. L. *Izv. Vysshikh Uch. Zav., Khim.i Khim. Tekhnol.* **1992**, *35*, 27. (d) Zhu, D.; Lu, J. *Sch. Chem. Eng.* **1990**, *19*, 735. (e) Tkach, V. S.; Shmidt, F. K.; Sergeeva, T. N.; Malakhova, N. D. *Neftekhimia* **1975**, *15*, 703. (f) Muthukumaru, P.; Ravindranathan, M.; Sivaram, S. *Chem. Rev.* **1986**, *86*, 353. (g) Skupinska, J. *Chem. Rev.* **1991**, *91*, 613.

(6) Keim, W.; Kowalt, F. H.; Goddard, R.; Kruger, C. *Angew. Chem., Int. Ed. Engl.* **1978**, *17*, 466.

(7) (a) Klabunde, U.; Ittel, S. D. *J. Mol. Catal.* **1987**, *41*, 123. (b) Klabunde, U.; Mülhaupt, R.; Herskovitz, T.; Janowicz, A. H.; Calabrese, J.; Ittel, S. D. *J. Polym. Sci., Part A: Polym. Chem.* **1987**, *25*, 1989.

(8) (a) Johnson, L. K.; Killian, C. M.; Brookhart, M. *J. Am. Chem. Soc.* **1995**, *117*, 6414. (b) Brookhart, M. S.; Johnson, L. K.; Killian, C. M.; Arthur, S. D.; Feldmann, J.; McCord, E. F.; Mchain, S. J.; Kreutzev, K. A.; Bennett, M. A.; Coughlin, E. B.; Ittel, S. D.; Parthasarathy, A.; Tempel, D. J. WO Patent Application to Du Pont, 9623010, April 3, 1995. (c) Johnson, L. K.; Mecking, S.; Brookhart, M. J. *Am. Chem. Soc.* **1996**, *118*, 267. (d) Killian, C. M.; Tempel, D. J.; Johnson, L. K.; Brookhart, M. *J. Am. Chem. Soc.* **1996**, *118*, 11664. (e) Mecking, S.; Johnson, L. K.; Wang, L.; Brookhart, M. *J. Am. Chem. Soc.* **1998**, *120*, 888.

(9) Johnson, L.; Bennett, A.; Dobbs, K.; Hauptman, E.; Ionkin, A.; Ittel, S.; McCord, E.; McLain, S.; Radzewich, C.; Yin, Z.; Wang, L.; Wang, Y.; Brookhart, M. *Polym. Mater. Sci. Eng.* **2002**, *86*, 319.

(10) (a) Wang, C.; Friedrich, S.; Younkin, T. R.; Li, R. T.; Grubbs, R. H.; Bansleben, D. A.; Day, M. W. *Organometallics* **1998**, *17*, 3149. (b) Younkin, T. R.; Conner, E. F.; Henderson, J. I.; Friedrich, S. K.; Grubbs, R. H.; Bansleben, D. A. *Science* **2000**, *287*, 460. (c) Connor, E. F.; Younkin, T. R.; Henderson, J. I.; Hwang, S.; Grubbs, R. H.; Roberts, W. P.; Litzau, J. J. *J. Polym. Sci., Part A: Polym. Chem.* **2002**, *40*, 2842. (d) Connor, E. F.; Younkin, T. R.; Henderson, J. I.; Waltman, A. W.; Grubbs, R. H. *Chem. Commun.* **2003**, 2272.

(11) (a) Gibson, V. S.; Tomov, A.; White, A.; Williams, D. J. *Chem. Commun.* **2001**, 719. (b) Gibson, V. S.; Tomov, A. *Chem. Commun.* **2001**, 1964.

(12) (a) Hicks, F. A.; Brookhart, M. *Organometallics* **2001**, *20*, 3217. (b) Hicks, F. A.; Jenkins, J. C.; Brookhart, M. *Organometallics* **2003**, *22*, 3533. (c) Jenkins, J. C.; Brookhart, M. *J. Am. Chem. Soc.* **2004**, *126*, 5827.

(13) Jenkins, J. C.; Brookhart, M. *Organometallics* **2003**, *22*, 250.

(14) (a) Desjardins, S. Y.; Cavell, K. J.; Jin, H.; Skelton, B. W.; White, A. H. *J. Organomet. Chem.* **1996**, *515*, 233. (b) Desjardins, S. Y.; Cavell, K. J.; Hoare, J. L.; Skelton, B. W.; Sobolev, A. N.; White, A. H.; Keim, W. *J. Organomet. Chem.* **1997**, *554*, 163.

(15) Rachita, M. J.; Huff, R. L.; Bennett, J. L.; Brookhart, M. *J. Polym. Sci., Part A: Polym. Chem.* **2000**, *38*, 4627.

(16) Schröder, D. L.; Keim, W.; Zuideveld, M. A.; Mecking, S. *Macromolecules* **2002**, *35*, 6071.

(17) (a) Wiencko, H. L.; Kogut, E.; Warren, T. H. *Inorg. Chim. Acta* **2003**, *345*, 199. (b) Zhou, M.-S.; Huang, S.-P.; Weng, L.-H.; Sun, W.-H.; Liu, D.-S. *J. Organomet. Chem.* **2003**, *665*, 237. (c) Zhang, D.; Jin, G.-X.; Weng, L.-H.; Wang, F. *Organometallics* **2004**, *23*, 3270. (d) Bourget-Merle, L.; Lappert, M. F.; Severn, J. R. *Chem. Rev.* **2002**, *102*, 3031. (e) Gao, H.; Guo, W.; Bao, F.; Gui, G.; Zhang, J.; Zhu, F.; Wu, Q. *Organometallics* **2004**, *23*, 6273.

(18) Zhang, D.; Jin, G.-X. *Organometallics* **2003**, *22*, 2851.

(19) Sun, W.-H.; Zang, W.; Gao, T.; Tang, X.; Chen, L.; Li, Y.; Jin, X. *J. Organomet. Chem.* **2004**, *689*, 917.

(20) Avent, A. G.; Hitchcock, P. B.; Lappert, M. F.; Sablong, R.; Severn, J. R. *Organometallics* **2004**, *23*, 2591.

(21) (a) Arndt, M.; Gosmann, M. *Polym. Bull.* **1998**, *41*, 433. (b) Zhao, C.-T.; Ribeiro, M. R.; Portela, M. F.; Pereira, S.; Nunes, T. *Eur. Polym. J.* **2001**, *37*, 45.

(22) Lee, B. Y.; Kim, Y. H.; Shin, H. J.; Lee, C. H. *Organometallics* **2002**, *21*, 3481.

(23) Li, Y.-S.; Li, Y.-R.; Li, X.-F. *J. Organomet. Chem.* **2003**, *667*, 185.

(24) Borkar, S.; Saxena, P. K. *Polym. Bull.* **2000**, *44*, 167.

(25) Yang, H.; Sun, W.-H.; Chang, F.; Li, Y. *Appl. Catal. A: Gen.* **2003**, *252*, 261.

sen for the reactivity study case.[26] In addition, we present preliminary results on the polymerization of norbornene, the dimerization of propylene, and the oligomerization of ethylene catalyzed by nickel(II) benzamidinate complexes.

Experimental Section

General Methods. All manipulations were performed with the exclusion of oxygen and moisture using flamed Schlenk-type glassware on a dual-manifold Schlenk line or interfaced to a high-vacuum (10^{-5} Torr) line. For storage of air-sensitive materials, a nitrogen-filled Vacuum Atmospheres glovebox with a medium-capacity recirculator (1−2 ppm O_2) was used. NMR spectra were recorded on Bruker AM-300 and AM-500 spectrometers. Chemical shifts for ^{1}H NMR and ^{13}C NMR were referenced to internal solvent resonances and reported relative to tetramethylsilane. The NMR experiments of the complexes were conducted in Teflon valve sealed tubes after vacuum transfer of the solvent in a high-vacuum line. The NMR characterization of polynorbornenes was performed in deuterated 1,1,2,2-tetrachloroethane at 130 °C. Molecular weights of polymers were determined by the GPC method on a Waters-Alliance 2000 instrument using 1,2,4-trichlorobenzene (HPLC) as the mobile phase at 150 °C.

Low-temperature X-ray diffraction experiments were carried out on a Nonius-KappaCCD diffractometer with graphite-monochromatized Mo Kα radiation. The crystals were placed in dry and degassed Parathon-N (DuPont) oil in a glovebox. Single crystals were mounted on the diffractometer under a stream of cold N_2 at 230 K. Cell refinements and data collection and reduction were carried out with the Nonius software package.[27] The structure solution was carried out by the SHELXS-97[28] and SHELXSL-97[29] software packages. The ORTEP program incorporated in the TEXRAY structure analysis package was used for molecular graphics.[30]

The electronic spectra were recorded on a HP 8452A diode array spectrophotometer. GC analysis was conducted on a Varian CP-3800 instrument with a DB-5 type capillary column of 30 m length and 0.25 mm internal diameter. GS/MS analysis was performed on a Finnigan MAT TSQ 70 mass spectrometer. FTIR spectra were registered using a Bruker Vector 22 instrument.

Materials. Argon and nitrogen were purified by passage through an MnO oxygen removal column and a Davison 4 Å molecular sieves column. Analytically pure solvents were distilled under argon from Na/K alloy (diethyl ether, hexane), Na (toluene), P_2O_5 (dichloromethane), or BaO (pyridine). All solvents for vacuum line manipulations were stored under vacuum over Na/K alloy. Nitrile compounds (Aldrich) and TMEDA (*N*,*N*,*N*′,*N*′-tetramethylethylenediamine) were degassed and freshly distilled under argon. Methylalumoxane (Witco) was prepared from a 30% suspension in toluene by vacuum evaporation of the solvent at 25 °C/10^{-5} Torr. MeLi·LiBr, MeMgBr, Ni(acac)$_2$, (DME)NiBr$_2$, LiN(SiMe$_3$)$_2$, and norbornene (bicyclo[2.2.1]hept-2-ene) were purchased and used as received (Aldrich). Et_3NHCl (Aldrich) was sublimated under vacuum at 200 °C.

The lithium benzamidinate complexes PhC(NSiMe$_3$)$_2$Li(TMEDA) (**1a**) and *p*-MePhC(NSiMe$_3$)$_2$Li(TMEDA) (**1b**),[31] (TMEDA)Ni((acac)$_2$ (**2**),[32] (TMEDA)MgMe$_2$,[33] and (TMEDA)NiMe$_2$[10d,32a] were prepared according to the literature procedures.

Synthesis of PhC(NSiMe$_3$)$_2$Ni(acac) (3) and PhC(NSiMe$_3$)$_2$Ni(acac)(TMEDA) (4). To a well-stirred solution of complex **2** (3.20 g, 8,58 mmol) in 40 mL of toluene was added 3.32 g (8.58 mmol) of ligand **1a**. A color change from turquoise to a deep violet was observed. The resulting mixture was stirred for 10 h at room temperature and filtered cold. Slow cooling of this solution for 50 h at −40 °C provided a mixture of fine ruby red **3** and emerald green **4** crystals. The mixture was filtered through a frit and evaporated under vacuum. Repeated washing of the crystal mixture with toluene allowed the full removal of TMEDA from complex **4**, forming complex **3** in 66% yield as the sole product. Anal. Calcd for $C_{18}H_{30}N_2O_2Si_2Ni$ (421.31): C, 51.31; H, 7.18; N, 6.65. Found: C, 51.52; H, 7.41; N, 7.01. Mp: 75 °C. UV/vis (toluene): λ_{max} 500 nm.

When the obtained mixture of complexes **3** and **4** was washed with TMEDA, complex **4** was obtained in 63% yield. Anal. Calcd for $C_{24}H_{46}N_4NiO_2Si_2$ (537.51): C, 53.63; H, 8.63; N, 10.42. Found: C, 53.52; H, 8.41; N, 10.01. Mp: 89 °C dec.

Synthesis of [PhC(NSiMe$_3$)$_2$]$_2$Ni$_2$(I) (5). A 1.2 g amount (2.85 mmol) of complex **3** was dissolved in 30 mL of diethyl ether, and 2.59 mL of a 1.1 M solution of methyllithium in hexane (2.85 mmol) was added dropwise at −78 °C. The reaction mixture was warmed to 0 °C and stirred for 3 h, and the solvent was evaporated under vacuum. A 30 mL portion of hexane was vacuum-transferred to the residue, and LiCl was removed by filtration. Cooling the solution to −40 °C overnight resulted in the formation of orange-brown crystals of (benzamidinate)nickel dimer complex, which was found not to be stable at room temperature and instead disproportionated to metallic nickel and the bis[bis(trimethylsilyl)benzamidinate]nickel complex **6**. The X-ray structure was possible to determine because the decomposition of complex **5** was rather slow at 220 K.

Synthesis of the Complex (TMEDA)$_2$Ni(0) (7). A 0.25 g portion (1.47 mmol) of (TMEDA)MgMe$_2$ was added to a cooled (−30 °C) solution of complex **3** (0.62 g, 1.47 mmol) in diethyl ether. The resulting mixture was warmed to −10 °C and stirred at this temperature for 4 h, and the solvent was evaporated. A 20 mL portion of toluene was vacuum-transferred to the residue, and Mg(acac)(PhC(NTMS)$_2$) was removed by filtration. Cooling the solution to −40 °C for 1 week resulted in the formation of brown crystals of (TMEDA)$_2$Ni(0) in 43% yield.

Synthesis of *p*-MePhC(NSiMe$_3$)$_2$Ni(acac) (8), *p*-MePhC(NSiMe$_3$)$_2$Ni(acac)(TMEDA) (9), and [*p*-MePhC(NSiMe$_3$)$_2$]$_2$Ni (10). In a manner similar to that described for the preparation of complexes **3** and **4**, 2.33 g (6.24 mmol) of complex **2** was dissolved in 40 mL of toluene and reacted with 2.50 g (6.24 mmol) of ligand **1b.** The resulting mixture was stirred at room temperature for 10 h, producing a dark violet solution. After the solution was filtered and cooled to −50 °C for 50 h, a mixture (2.5 g) of fine bright red (**8**), green (**9**), and violet (**10**) crystals were obtained. The mixture of complexes was filtered and dried under vacuum. Multiple fractional

(26) (a) Wedler, M.; Recknagel, A.; Giljc, J. W.; Noltemeyer, M.; Edelmann, F. T. *J. Organomet. Chem*. **1992**, *426*, 295. (b) Barker, J.; Kilner, M. *Coord. Chem. Rev*. **1994**, *133*, 219. (c) Cotton, F. A.; Matonic, J. H.; Murillo, C. A. *Inorg. Chem*. **1995**, *35*, 498. (d) Edelmann, F. T. *Coord. Chem. Rev*. **1994**, *137*, 403 and references therein. (e) Volkis, V.; Shmulinson, M.; Averbuj, C.; Lisovskii, A.; Edelmann, F. T.; Eisen, M. S. *Organometallics* **1998**, *17*, 3155.

(27) KappaCCD Collect Program for data collection and HKL and Scalepack and Denzo (Otwinowski and Minor, 2001) software package for data reduction and cell refinement; Enraf-Nonius, Delft, The Netherlands, 2001.

(28) Sheldrick, G. M. *Acta Crystallogr*. **1990**, *A46*, 467.

(29) Sheldrick, G. M. SHELXL-97, Program for the Refinement of Crystal Structures; University of Göttingen, Göttingen, Germany, 1997.

(30) ORTEP, TEXRAY Structure Analysis Package; Molecular Structure Corp., 3200 Research Forest Drive, The Woodlands, TX 77381, 1999.

(31) (a) Dick, D. G.; Duchateau, R.; Edema, J. J. H.; Gambarotta, S. *Inorg. Chem.* **1993**, *32*, 1959. (b) Volkis, V.; Nelkenbaum, E.; Lisovskii, A.; Hasson, G.; Semiat, R.; Kapon, M.; Botoshansky, M.; Eishen, Y.; Eisen, M. S. *J. Am. Chem. Soc*. **2003**, *125*, 2179.

(32) (a) Kaschube, W.; Porschke, K. R.; Wilke, G. *J. Organomet. Chem.* **1988**, *355*, 525. (b) Zeller, A.; Herdtweck, E.; Strassner, Th. *Inorg. Chem. Commun.* **2004**, 7, 296.

(33) (a) Salinger, R.; Mosher, H. S. *J. Am. Chem. Soc.* **1964**, *86*, 1782. (b) Coates, G. E.; Heslop, J. A. *J. Chem. Soc. A* **1966**, 26.

precipitation allows us to obtain in very low yields the complexes for X-ray determination. Anal. Calcd for complex **8**, $C_{19}H_{32}N_2NiO_2Si_2$ (435.36): C, 52.37; H, 7.35; N, 6.43. Found: C, 51.82; H, 7.46; N, 6.11. Anal. Calcd for complex **9**, $C_{25}H_{48}N_4NiO_2Si_2$ (551.56): C, 52.21; H, 8.70; N, 10.15. Found: C, 53.52; H, 8.43; N, 10.42. Anal. Calcd for complex **10**, $C_{28}H_{50}N_4NiSi_2$ (613.78): C, 54.74; H, 8.15; N, 9.12. Found: C, 54.25; H, 8.37; N, 8.93.

Synthesis of $NiMe_2Py_2$ (11). To a cooled (−70 °C) diethyl ether solution (5 mL) of (TMEDA)$NiMe_2$ prepared by the reaction of (TMEDA)Ni(acac)$_2$ (1.18 g, 3.16 mmol) with 0.54 g (3.16 mmol) of (TMEDA)$MgMe_2$ was added 5 mL of pyridine. The reaction mixture was stirred at this temperature for 15 min and then for 4 h at 0 °C, producing a deep red solution. After partial evaporation of toluene, the solution was cooled to −40 °C overnight to obtain red-brown crystals, which were characterized by low-temperature X-ray diffraction analysis. $NiMe_2Py_2$ was found to be unstable and decomposes, yielding black Ni(0) in solution within $t_{1/2}$ = 45−60 min at room temperature.

Synthesis of *p*-MePhC(NSiMe$_3$)(NHSiMe$_3$) (12). A 0.86 g portion (6.24 mmol) of Et_3NHCl was added to a solution of the ligand **1b** (2.5 g, 6.24 mmol) in 30 mL of toluene. The mixture was stirred at room temperature for 20 h. The solution was isolated via filtration through Celite, and the solvent was evaporated under vacuum, producing a transparent yellow oil. The product was washed with an additional 25 mL of toluene and dried under vacuum overnight to obtain 1.2 g (81%) of ligand **12** as a viscous oil. Anal. Calcd for $C_{14}H_{26}N_2Si_2$ (278.16): C, 60.43; H, 9.35; N, 10.07. Found: C, 60.89; H, 9.15; N, 10.55. ^{1}H NMR (C_6D_6, 300 MHz): δ 7.16 (d, ^3J = 8 Hz, 2H, Ph), 6.91 (d, ^3J = 8 Hz, 2H, Ph), 4.25 (s, 1H, HN), 2.09 (s, 3H, CH_3Ph), 0.26 (s, 9H, Si(CH$_3$)$_3$), 0.16 (s, 9H, Si(CH$_3$)$_3$). ^{13}C NMR (C_6D_6, 75 MHz): δ 162.8 (NC=N), 138.3, 137.7, 128.0, 125.8, (Ph), 20.3 (CH_3Ph), 1.1 (Si(CH$_3$)$_3$), −1.0 (Si(CH$_3$)$_3$).

Synthesis of [*p*-MePhC(NSiMe$_3$)]$_2$Ni(Py) (14). (TMEDA)-$NiMe_2$ prepared by the reaction of (TMEDA)Ni(acac)$_2$ (0.22 g, 0.59 mmol) with 0.10 g (0.59 mmol) of (TMEDA)$MgMe_2$ was dissolved in 10 mL of a cooled (−70 °C) solution mixture of toluene and pyridine (3:1) and reacted with a toluene solution (3 mL) of ligand **12** (0.145 g, 0.50 mmol). The resulting mixture was warmed to −20 °C and stirred at this temperature for 15 min and then for 3 h at room temperature, giving a deep red solution. Bubbling was observed. Initially, the reaction produces the expected methyl complex **13**, which could be observed by following the crude reaction in the NMR: ^{1}H NMR δ −0.25 (Ni−CH_3); ^{13}C NMR (C_6D_6) δ −8.0. However, after repeated washing of the precipitated complex with cold toluene and recrystallization at −30 °C for 2 weeks, green single crystals of complex **14** have been obtained in 14% yield. The molecular structure of complex **14** was determined by low-temperature X-ray crystallography. Anal. Calcd for $C_{33}H_{55}N_5NiSi_4$ (692.86): C, 57.21; H, 8.00; N, 10.11. Found: C, 57.80; H, 8.14; N, 10.45.

Norbornene Polymerization Procedure. The catalytic polymerization of norbornene was studied using complex **3** activated with MAO. A 50 mL three-necked polymerization bottle, equipped with a sidearm Schlenk tube for the addition of solids and a stirrer, was charged inside a glovebox with a certain amount of MAO and 0.5 g of norbornene. The bottle was connected to a Schlenk vacuum line and, after introduction of a toluene solution of the precatalyst under an argon flow via a syringe and stirring of the catalytic mixture for 5 min, the monomer was added in one portion from the sidearm. After being stirred for a desired amount of time, the reaction mixture was poured into acidified methanol (1:4) in order to quench the polymerization. The resulting precipitated polymer was separated by filtration, washed with water and acetone several times, and finally dried under vacuum at 70 °C. The polynorbornene yield in percentage was calculated as the weight fraction of converted monomer over the total monomer.

General Procedure for the Dimerization of Propylene. Experiments at higher pressures were performed in a 100 mL stainless steel reactor. The reactor was charged inside a glovebox with a certain amount of the catalytic precursor, MAO, and a magnetic stirrer. The reactor was connected to a high-vacuum line, evacuated under vacuum, and frozen at liquid nitrogen temperature. A 25 mL portion of liquid propylene was vacuum-transferred to the frozen reactor. The reactor was rapidly warmed to room temperature and the solution stirred. After being stirred for a certain period, the mixture was quenched by exhausting the unreacted propylene. An aliquot of the reaction mixture was removed for GLC analysis, whereas a set of 10 different hexenes was used as internal reference.

Ethylene Oligomerization. The catalytic oligomerization of ethylene activated by complex **3** and MAO was performed in 100 mL stainless steal reactors. The reactor was charged inside a glovebox with a certain amount of the catalytic precursor, MAO, and a magnetic stirrer. The reactor was connected to a high-vacuum line, and, after introduction of the solvent (10 mL) under an argon flow, it was frozen at liquid nitrogen temperature and evacuated under vacuum. The reactor was then warmed to room temperature, pressurized to 30 bar of ethylene pressure, and stirred for the desired reaction time. The reaction temperature was maintained using an external water−ice bath to control the reaction exotherm. After 1 h the reaction was stopped by cooling the reactor to −15 °C and depressurizing. The contents were transferred into a cold tared 50 mL heavy duty Schlenk flask, sealed, and weighed. The oligomers obtained were analyzed by GC/MS.

Results and Discussion

We begin the presentation of the results with the synthesis of our starting materials followed by the synthesis of the complexes and we end the presentation by describing some of the catalytic reactions. The ligands used in this study are the lithium benzamidinates PhC(NSiMe$_3$)$_2$Li(TMEDA) (**1a**) and *p*-MePhC-(NSiMe$_3$)$_2$Li(TMEDA) (**1b**).[31] Since the use of Ni(acac)$_2$ as the Ni(II) precursor showed very little reactivity in our hands, we decided to use the more reactive (TMED-A)Ni(acac)$_2$ (**2**), following the Wilke procedure.[32]

Synthesis of the Nickel(II) *N,N′*-Bis(trimethylsilyl)benzamidinate Acetylacetonate Complexes 3 and 4. Reaction of complex **2** with an equimolar amount of the ancillary ligand **1a** in toluene at ambient temperature afforded a mixture of the compounds PhC-(NSiMe$_3$)$_2$Ni(acac) (**3**) PhC(NSiMe$_3$)$_2$Ni(acac)(TMEDA) (**4**) in a moderate yield (75%; eq 1).

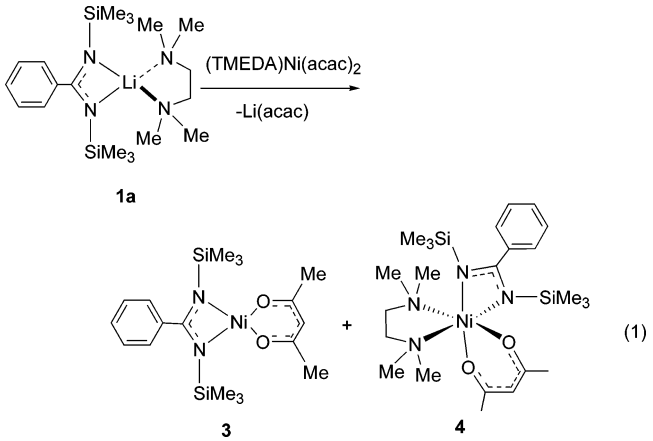

(1)

These two complexes were separated by fractional precipitation from toluene and recrystallized to obtain

Table 1. Crystal Data and Details of Data Collection for Complexes 3−5

	3	4	5
empirical formula	$C_{18}H_{30}N_2NiO_2Si_2$	$C_{24}H_{46}N_4NiO_2Si_2$	$C_{26}H_{46}N_4Ni_2Si_4$
formula wt	421.33	537.54	644.45
temp (K)	230.0(1)	230.0(1)	230.0(1)
wavelength (Å)	0.710 70	0.710 70	0.710 73
cryst syst, space group	monoclinic, $P2_1/c$	monoclinic, $P2_1/c$	triclinic, $P\bar{1}$
unit cell dimens			
a (Å)	15.8990(6)	10.8590(2)	11.3643(5)
b (Å)	6.8500(2)	13.9810(3)	12.0823(6)
c (Å)	21.3210(9)	20.4510(6)	13.7054(7)
α (deg)	90	90	106.974(2)
β (deg)	96.5200(12)	101.0250(8)	108.096(2)
γ (deg)	90	90	91.455(2)
V (Å^3)	2307.01(15)	3047.56(12)	1696.84(14)
Z	4	4	2
D_{calcd} (mg/m^3)	1.213	1.172	1.261
μ (mm^{-1})	0.957	0.740	1.271
F(000)	896	1160	684
cryst size (mm)	0.08 × 0.12 × 0.30	0.15 × 0.20 × 0.32	0.05 × 0.08 × 0.15
θ range for data collecn (deg)	1.92−25.05	1.77−25.05	1.65−23.00
limiting indices	$0 \le h \le 18$	$0 \le h \le 12$	$-12 \le h \le 12$
	$0 \le k \le 8$	$0 \le k \le 16$	$-13 \le k \le 13$
	$-25 \le l \le 25$	$-24 \le l \le 23$	$-15 \le l \le 14$
no. of rflns collected/unique	4071/4071 (R(int) = 0.0000)	5382/5382 (R(int) = 0.0000)	8516/4715 (R(int) = 0.0869)
completeness to θ	25.05; 99.8%	25.05; 99.8%	23.00; 99.9%
refinement method	full-matrix least squares on F^2		
no. of data/restraints/params	4071/0/259	5382/0/470	4715/0/371
goodness of fit on F^2	1.026	1.054	0.914
final R indices ($I > 2\sigma(I)$)	R1 = 0.0432, wR2 = 0.0932	R1 = 0.0350, wR2 = 0.0805	R1 = 0.0561, wR2 = 0.0923
R indices (all data)	R1 = 0.0700, wR2 =0.1012	R1 = 0.0524, wR2 = 0.0851	R1 = 0.1279, wR2 = 0.1052
largest diff peak and hole (e Å^{-3})	0.275 and −0.221	0.495 and −0.296	0.703 and −0.318

single crystals, which were found suitable for X-ray measurements. Repeated washing of the crystal mixture with toluene allowed the full removal of the TMEDA, forming complex **3** in 66% yield as the sole product, or in contrast, the addition of TMEDA gave complex **4** as the sole product in similar yield (63%). Attempts to prepare these complexes from compound **2** and the lithium (trimethylsilyl)benzamidinate ligand without the coordinated TMEDA were unsuccessful.[34]

The crystal structure of complex **3** is presented in Figure 1. Crystallographic data and structure refinement details for the complex and selected bond lengths and angles are listed in Table 1 and Table 4, respectively. The low-temperature X-ray diffraction analysis reveals that the ruby red complex **3** contains one η^2 chelating benzamidinate and one η^2-acetylacetonate ligand around the nickel center, adopting a slightly distorted square planar coordination geometry (the sum of the angles around the Ni metal is 360.02°). The core units of complex **3** comprise a four-membered Ni−N−C−N ring and a six-membered Ni−O−C−C−C−O ring, with identical Ni−N bond lengths and comparable Ni−O bond lengths (see Table 4).

The four-membered ring is partially puckered, as shown by the small dihedral angle N(5)−C(6)−N(13)−Ni = 3.7° and the angles O(24)−Ni−N(5) = 166.78(10)° and O(18)−Ni−N(13) = 166.96(10)°. Interestingly, the Ni−N distances in **3** are shorter than in complex **2** (by ∼0.27 Å) due to the lower density of charge at the metal in the latter complex, which is involved in the chelating of the TMEDA ligand, as compared to the former complex, which has a higher positive charge, causing

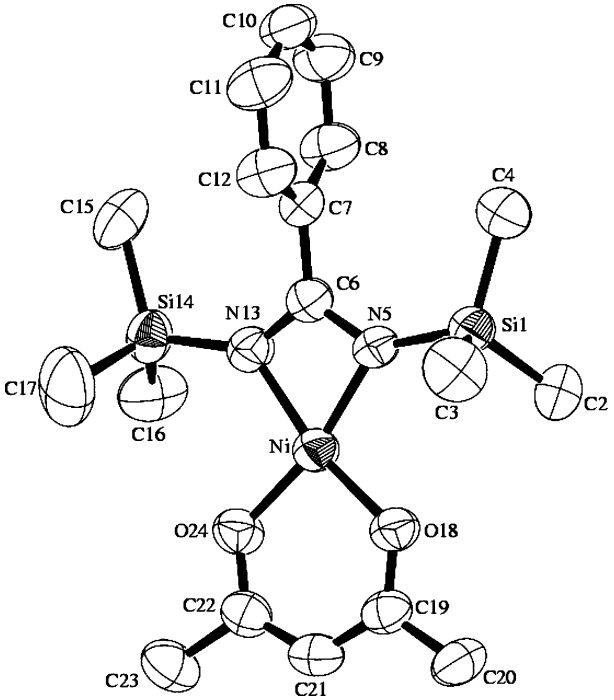

Figure 1. Molecular structure of complex **3**. Thermal ellipsoids are given at the 50% probability level.

the shorter bond lengths. Similarly, the Ni−O bond lengths, which are shorter in complex **3** than in complex **2** (by ∼0.2 Å), indicate the large difference between hard and soft ligands around the cationic Ni(II) center, inducing a more relaxed structure in the complex **2** and a more compressed structure in complex **3**.

Normally all square-planar complexes of nickel, which are low spin, have no unpaired electrons and therefore

(34) Lisovskii, A.; Botoshansky. M.; Eisen, M. S. *Dalton* **2001**, 1692.

Table 2. Crystal Data and Details of the Data Collection for Complexes 6−9

	6 (with $Li_2Br_2(TMEDA)_2$)	**7**	**8**	**9**
empirical formula	$C_{38}H_{78}Br_2Li_2N_8NiSi_4$	$C_6H_{16}N_2Ni_{0.5}$	$C_{19}H_{32}N_2NiO_2Si_2$	$C_{25}H_{48}N_4NiO_2Si_2$
formula wt	991.85	145.56	435.36	551.56
temp (K)	230.0(2)	230.0(2)	230.0(2)	230.0(2)
wavelength (Å)	0.710 73	0.710 73	0.710 73	0.710 73
cryst syst, space group	monoclinic, $P2_1/n$	monoclinic, $C2/c$	orthorhombic, $Pbca$	monoclinic, $P2_1/c$
unit cell dimens				
a (Å)	11.5880(2)	8.5850(3)	17.6130(2)	14.9190(11)
b (Å)	15.1020(3)	14.3240(6)	12.8460(3)	10.9080(8)
c (Å)	32.8200(8)	10.0170(4)	20.9800(3)	20.112(2)
α (deg)	90	90	90	90
β (deg)	98.7610(8)	113.926(3)	90	103.606(3)
γ (deg)	90	90	90	90
V (Å^3)	5676.6(2)	1125.96(8)	4746.86(14)	3181.1(5)
Z	4	8	8	4
D_{calcd} (mg/m^3)	1.161	1.717	1.218	1.152
μ (mm^{-1})	1.864	1.707	0.932	0.711
F(000)	2088	640	1856	1192
cryst size (mm)	0.10 × 0.18 × 0.18	0.09 × 0.12 × 0.18	0.15 × 0.18 × 0.24	0.06 × 0.24 × 0.28
θ range for data collecn (deg)	1.26−23.00	2.84−24.97	1.94−25.05	1.40−25.04
limiting indices	$-12 \le h \le 12$	$-9 \le h \le 9$	$-20 \le h \le 20$	$-17 \le h \le 17$
	$-15 \le k \le 16$	$-16 \le k \le 16$	$-15 \le k \le 15$	$-11 \le k \le 12$
	$-36 \le l \le 35$	$-11 \le l \le 10$	$-24 \le l \le 24$	$-23 \le l \le 23$
no. of rflns collected/unique	13 399/7659 (R(int) = 0.0796)	2494/892 (R(int) = 0.0548)	7934/4200 (R(int) = 0.0232)	8874/5253 (R(int) = 0.0737)
completeness to θ	23.00; 96.9%	24.97; 90.7%	25.05; 100.0%	25.04; 93.7%
refinement method	full-matrix least squares on F^2			
no. of data/restraints/params	7659/0/496	892/0/80	4200/0/279	5253/0/307
goodness of fit on F^2	0.710	1.140	0.934	0.816
final R indices ($I > 2\sigma(I)$)	R1 = 0.0415, wR2 = 0.0816	R1 = 0.1050, wR2 = 0.3121	R1 = 0.0282, wR2 = 0.0775	R1 = 0.0647, wR2 = 0.1457
R indices (all data)	R1 = 0.1646, wR2 = 0.1199	R1 = 0.1579, wR2 = 0.3352	R1 = 0.0473, wR2 =0.0801	R1 = 0.1430, wR2 = 0.1582
largest diff peak and hole (e Å^{-3})	0.295 and −0.265	0.645 and −0.973	0.181 and −0.239	1.308 and −0.383

Table 3. Crystal Data and Data Collection Details for Complexes 10, 11, and 14

	10	**11**	**14**
empirical formula	$C_{14}H_{25}N_2Ni_{0.5}Si_2$	$C_{12}H_{16}N_2Ni$	$C_{33}H_{55}N_5NiSi_4$
formula wt	306.89	246.98	692.89
temp (K)	230.0(2)	230.0(2)	230.0(1)
wavelength (Å)	0.710 73	0.710 73	0.710 73
cryst syst, space group	monoclinic, $C2/c$	monoclinic, $C2/c$	monoclinic, $P2_1/n$
unit cell dimens			
a (Å)	26.7070(12)	9.809(2)	11.3360(2)
b (Å)	8.8830(6)	16.995(4)	12.1220(2)
c (Å)	20.4120(12)	15.197(3)	29.0420(5)
α (deg)	90	90	90
β (deg)	129.923(3)	99.037(10)	93.9240(8)
γ (deg)	90	90	90
V (Å^3)	3713.8(14)	2502.0(10)	3981.45(12)
Z	8	8	4
D_{calcd} (mg/m^3)	1.098	1.311	1.156
μ (mm^{-1})	0.672	1.521	0.635
F(000)	1320	1040	1488
cryst size (mm)	0.08 × 0.12 × 0.24	0.06 × 0.33 × 0.33	0.06 × 0.21 × 0.25
θ range for data collecn (deg)	1.99−25.05	2.40−25.04	1.41−25.05
limiting indices	$-31 \le h \le 31$	$0 \le h \le 11$	$-13 \le h \le 13$
	$-10 \le k \le 10$	$0 \le k \le 19$	$-14 \le k \le 14$
	$-24 \le l \le 24$	$-18 \le l \le 17$	$-34 \le l \le 34$
no. of rflns collected/unique	5976/3289 (R(int) = 0.0598)	2142/2142 (R(int) = 0.0000)	13 235/7050 (R(int) = 0.0405)
completeness to θ			
refinement method	25.05; 99.6%	25.04; 96.4%	25.05; 99.9%
no. of data/restraints/params	full-matrix least squares on F^2		
goodness of fit on F^2	3289/0/172	2142/0/158	7050/0/388
final R indices ($I > 2\sigma(I)$)	0.901	1.067	0.912
R indices (all data)	R1 = 0.0522, wR2 = 0.1343	R1 = 0.0500, wR2 = 0.1087	R1 = 0.0344, wR2 = 0.0818
largest diff peak and hole (e Å^{-3})	R1 = 0.1314, wR2 = 0.1482	R1 = 0.0976, wR2 =0.1214	R1 = 0.0734, wR2 = 0.1033
	0.336 and −0.189	0.246 and −0.257	369 and −0.453

show diamagnetic properties.[35] However, ^{1}H NMR spectroscopy reveals that complex **3** is paramagnetic, giving broad contact-shifted signals in the ranges of −15 to −4 and 60−90 ppm, indicating that a plausible equilibrium between the square-planar and the expected paramagnetic tetrahedral structure is operative in solution.[36]

The crystal structure of complex **4** is presented in Figure 2. Crystallographic data and structure refinement details for the complex and selected bond lengths

(35) Shriver, D. F.; Atkins, P. W.; Langford, C. H. *Inorganic Chemistry,* 2nd ed.; Oxford University Press: Oxford, U.K., 1998.

Table 4. Comparison of the Bond Lengths (Å) and Angles (deg) for Complexes 3, 4, 8, and 9

3		4		8		9	
			Bond Lengths				
Ni−N(5)	1.901(2)	Ni−N(5)	2.0955(17)	Ni−N(1)	1.8953(17)	Ni−N(1)	2.101(4)
Ni−N(13)	1.906(2)	Ni−N(13)	2.2147(18)	Ni−N(2)	1.9113(18)	Ni−N(2)	2.228(4)
Ni−O(24)	1.844(2)	Ni−O(18)	2.0272(16)	Ni−O(1)	1.8462(15)	Ni−O(1)	2.029(4)
Ni−O(18)	1.850(2)	Ni−O(24)	2.0311(16)	Ni−O(2)	1.8475(15)	Ni−O(2)	2.041(3)
		Ni−N(30)	2.1970(19)			Ni−N(3)	2.188(5)
		Ni−N(25)	2.2210(19)			Ni−N(4)	2.208(4)
			Bond Angles				
N(5)−Ni−N(13)	69.74(10)	N(5)−Ni−N(13)	63.56(7)	N(1)−Ni−N(2)	70.02(8)	N(1)−Ni−N(2)	63.96(16)
O(24)−Ni−N(5)	166.78(10)	O(24)−Ni−N(13)	161.00(6)	O(2)−Ni−N(1)	168.37(8)	O(2)−Ni−N(2)	161.24(15)
O(24)−Ni−O(18)	95.79(9)			O(1)−Ni−O(2)	96.10(7)	O(1)−Ni−O(2)	90.25(15)
O(18)−Ni−N(5)	97.38(9)	O(18)−Ni−N(5)	93.90(7(	O(1)−Ni−N(1)	95.53(7)		
O(24)−Ni−N(13)	97.05(10)			O(2)−Ni−N(2)	98.36(7)	O(1)−Ni− N(2)	86.18(15)
O(18)−Ni−N(13)	166.96(10)			O(1)−Ni−N(2)	165.54(7)	O(2)−Ni−N(1)	97.96(16)
		N(5)−Ni−N(30)	94.85(7)			N(4)−Ni−N(2)	95.44(17)
		O(18)−Ni− N(25)	88.99(7)			O(2)−Ni− N(4)	90.82(17)
		N(30)−Ni−N(25)	81.99(8)				

Table 5. Comparison of the Bond Lengths (Å) and Angles (deg) for Complexes 10, 6, Ni(II),[40] and 14

10		6		Ni(II)[40]		14	
			Bond Lengths				
Ni−N(2)	1.990(3)	Ni−N(5)	1.969(5)	Ni−N(4)	2.009(3)	Ni−N(4)	2.050(2)
Ni−N(1)	2.019(3)	Ni−N(13)	2.045(6)	Ni−N(3)	2.016(3)	Ni−N(3)	2.104(2)
Ni−N(2)#1	1.990(3)	Ni−N(30)	2.000(5)	Ni−N(1)	2.007(3)	Ni−N(2)	2.063(2)
Ni−N(1)#1	2.019(3)	Ni−N(22)	2.004(5)	Ni−N(2)	2.016(3)	Ni−N(1)	2.083(2)
			Bond Angles				
N(2)−Ni−N(1)	67.65(13)	N(5)−Ni−N(13)	68.6(2)	N(1)−Ni−N(2)	67.35(14)	N(2)−Ni−N(1)	65.59(9)
N(1)#1−Ni−N(1)	115.2(2)	N(30)−Ni−N(13)	121.5(3)	N(1)−Ni−N(3)	120.8(2)	N(4)−Ni−N(2)	105.53(9)
N(2)−Ni−N(1)#1	125.36(14)	N(5)−Ni−N(30)	137.1(2)	N(1)−Ni−N(4)	133.8(2)	N(2) −Ni−N(3)	106.79(9)
N(2)#1−Ni−N(1)	125.36(14)	N(22)−Ni−N(13)	118.9(2)	N(2)−Ni−N(3)	120.7	N(4)−Ni−N(1)	115.68(9)
N(2)−Ni−N(2)#1	158.7(2)	N(5)−Ni−N(22)	148.0(3)	N(2)−Ni−N(4)	152.3	N(1)−Ni−N(3)	172.38(8)
C(11)−Ni−C(11)#1	152.8(2)	C(23)−Ni−C(6)	159.3(3)	C(1)−Ni−C(14)	159.4(2)		

and angles, are listed in Tables 1 and 4, respectively. The emerald green complex crystallizes with the metal having a distorted-octahedral geometry. η^2-Benzamidinate, η^2-acetylacetonate, and η^2-TMEDA comprise the three ligands around the metal. The axial position is occupied by one oxygen and a nitrogen from the benzamidinate ligand with a transaxial angle of O(24)−Ni−N(13) = 161.00(6)°, whereas the second oxygen atom O(18), and the nitrogen atoms N(5), N(25), and N(30) occupy the equatorial position with the sum of the equatorial angles of 359.72°. The benzamidinate ligand is more puckered (N(5)−C(6)−N(13)−Ni = 10.0°) than in complex **3,** due to the steric hindrance between the methyl groups of the trimethylsilyl moiety and the acetylacetonate ligand. The bond lengths between the metal center and the amidinate nitrogen atoms are distinct, due to the difference in the static trans effects between the axial oxygen and the equatorial amine of the TMEDA ligand. Interestingly, this effect is less pronounced among the nitrogen atoms of the coordinative TMEDA ligands. Comparison of the M−N bond lengths of the amidinate complexes **4** and **3** and the M−N(TMEDA) bond lengths among complexes **4** and **2** shows that in complex **4** the M−N(amidinate) bonds are longer than those in complex **3**, whereas the M−N(TMEDA) bond lengths are alike. This result is in agreement with regard to the role of the TMEDA, implicating that its absence induces a more compressed structure with shorter bond lengths. In addition, with regard to the M−O bond lengths of the acac ligation, a similar compression effect is observed. In complex **4** the M−O bond lengths are longer than in complex **3** and similar to those in complex **2**.

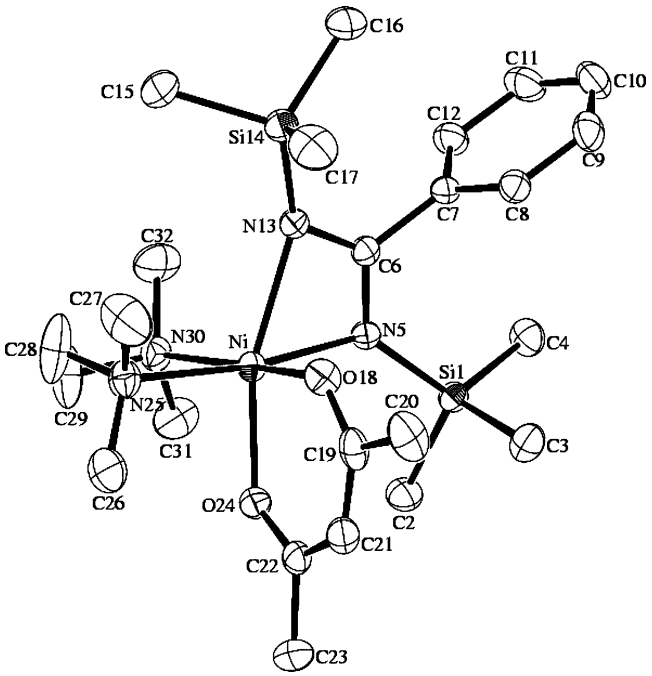

Figure 2. Crystal structure of complex **4**. Thermal ellipsoids are given at the 50% probability level.

Synthesis of the (μ_2,μ_2-*N*,*N*′-Bis(trimethylsilyl)-benzamidinate)nickel(I) Dimer 5. In an attempt to

(36) (a) Hayter, R. G.; Humiec, F. S. *Inorg. Chem.* **1965**, *4*, 1701. (b) Dori, Z.; Gray, H. B. *J. Am. Chem. Soc.* **1966**, *88*, 1394. (c) Frömmel, T.; Peters, W.; Wunderlich, H.; Kuchen, W. *Angew. Chem., Int. Ed. Engl.* **1993**, *32*, 907. (d) La Mar, G. N., Horrocks, W. DeW., Holm, R. H., Eds. *NMR of Paramagnetic Molecules*; Academic Press: New York and London, 1973.

replace the acetylacetonate ligand with an alkyl group, we have reacted complex **3** with MeLi·LiBr in an ether solution at low temperature. Instead of a methyl benzamidinate nickel compound being produced, a reduced orange (benzamidinate)nickel dimer, complex **5**, was obtained almost quantitatively (eq 2).

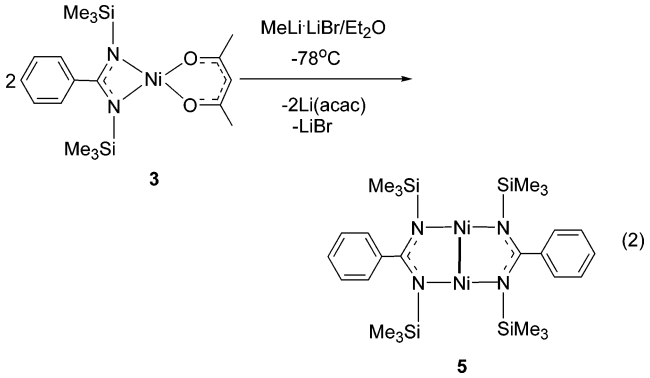

(2)

The low-temperature X-ray crystal structure of complex **5** is presented in Figure 3. Crystallographic data and structure refinement details for the complex are given in Table 1. The core units of complex **5** are the two five-membered Ni−N−C−N−Ni rings, which are slightly tilted, to produce a "figure eight" shape (N(5)−Ni(1)−Ni(2)−N(13) = 13.5°). Both five-membered rings are disposed in the same way with almost symmetrical M−N and N−C bond lengths (Ni(1)−N(5) = 1.874(5) Å, Ni(1)−N(18) = 1.876(5) Å, Ni(2)−N(30) = 1.868(5) Å, Ni(2)−N(13) = 1.876(5) Å, N(5)−C(6) = 1.328(8) Å, C(6)−N(13) = 1.336(7) Å, N(18)−C(23) = 1.339(6) Å, C(23)−N(30) = 1.348(8) Å). By comparison to other late-transition-metal binuclear benzamidinate-bridged compounds, the Ni−Ni distance (Ni(1)−Ni(2) = 2.2938(12) Å) is significantly shorter than in the analogous silver(I) (2.655 Å),[37] gold(I) (2.644 Å),[37] and copper(I) (2.424 Å)[38] complexes and in the palladium amidinate complex (μ-dpd)$_2$[Pd(dpd)]$_2$ (dpd = *N*,*N*′-diphenylbenzamidinate) (2.900 Å).[39] When the angles are compared among the different complexes, the angle N(5)−Ni−N(18) = 179.6(2)° in complex **5** is much larger, while the angle N(5)−C(6)−N(13) = 122.1(6)° is somewhat smaller, than in the corresponding Ag(I) (170.10(9) and 125.3(2)°), Au(I), (169.1(4) and 126.3(8)°), and Cu(I) (175.7(3) and 124.1°) complexes.

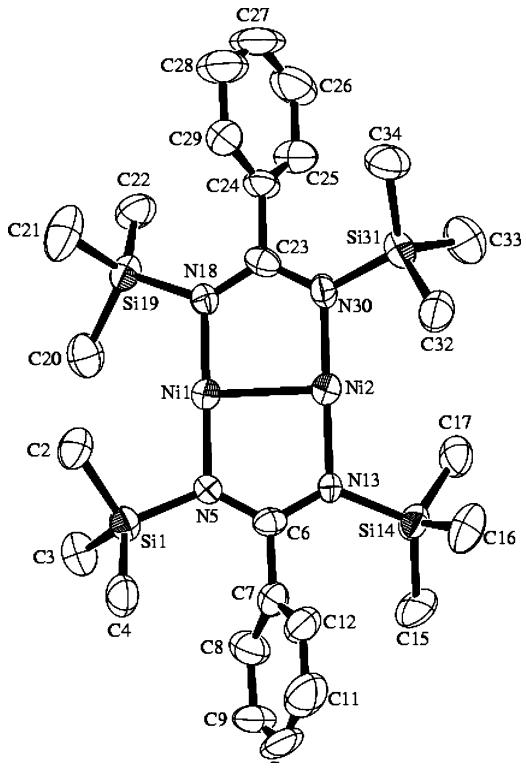

Figure 3. Crystal structure of complex **5**. Thermal ellipsoids are given at the 50% probability level.

Complex **5** was found not to be stable in solution at room temperature and to disproportionate to metallic nickel and the tetrahedral bis[bis(trimethylsilyl)benzamidinate]nickel complex **6** (eq 3). Complex **6** was also

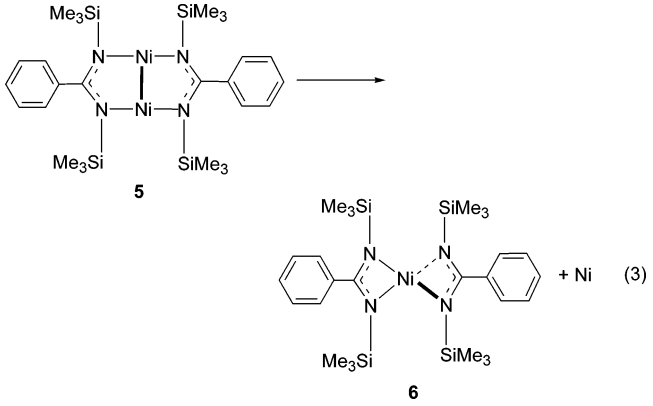

(3)

synthesized following the reaction of equimolar amounts of the ligand **1a** and (DME)NiBr$_2$ (DME = 1,2-dimethoxyethane) in ether (eq 4).

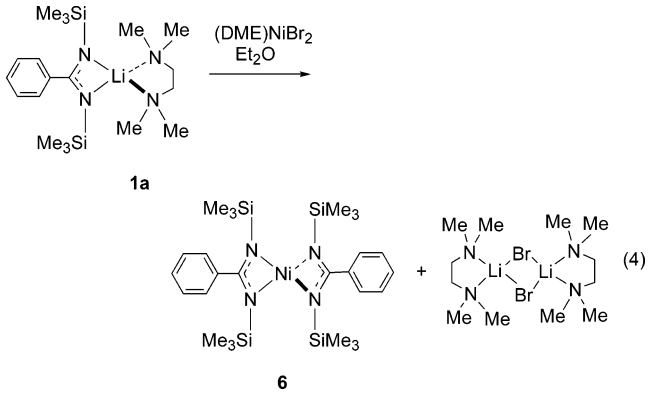

(4)

Low-temperature X-ray analysis shows that complex **6** crystallizes as a molecular complex containing one molecule of $Li_2Br_2(TMEDA)_2$. The molecular structure of complex **6** is presented in Figure 4a, whereas crystallographic data and structure refinement details are listed in Table 2 and selected bond lengths and angles are presented in Table 5. The Ni−N bond lengths in complex **6** were found to be not significantly different from those in the reported bis(benzamidinate)nickel complex (the reported values are also given in Table 5).[40] The reported complex was prepared by the reaction of

(37) Fenske, D.; Baum, G.; Zinn, A.; Dehnicke, K. *Z. Naturforsch.*, *B* **1990**, *45*, 1273.
(38) Maier, S.; Hiller, W.; Straehle, J.; Ergezinger, C.; Dehnicke, K. *Z. Naturforsch.*, *B* **1988**, *43*, 1628.
(39) Yao, C.-L.; He, L.-P.; Korp, J. D.; Bear, J. L. *Inorg. Chem.* **1988**, *27*, 4389.

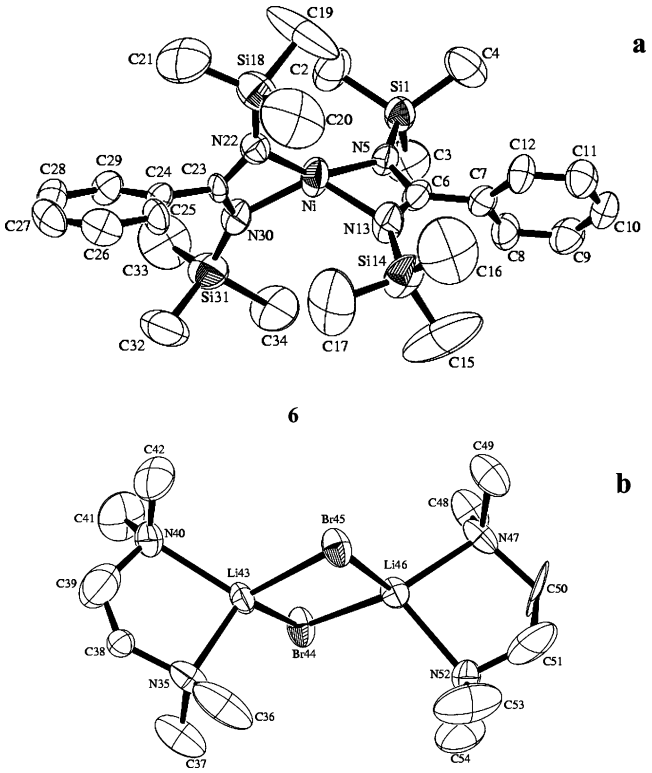

Figure 4. ORTEP diagrams of complex **6** (a) and the cocrystallized $Li_2Br_2(TMEDA)_2$ salt (b). Thermal ellipsoids are given at the 50% probability level.

the (*N*,*N*′-bis((trimethylsilyl)benzamidinate)Mg(thf)$_2$ complex with $NiBr_2$(thf), revealing a distorted-tetrahedral environment around the Ni(II) ion. The bent vector along the central ipso carbons C(23)−Ni−C(6) and the angles N(5)−Ni−N(13) and N(30)−Ni−N(13) in complex **6** are similar to those exhibited in the reported Ni(II) compound (C(1)−Ni−C(14), N(1)−Ni−N(2), and N(1)−Ni−N(3), respectively), although there are some differences observed in their interligand angles (N(5)−Ni−N(30) = 137.1(2)° and N(5)−Ni−N(22) = 148.0(3)° for complex **6** and N(1)−Ni−N(4) = 133.8(2)° and N(2)−Ni−N(4) = 152.3° for the reported complex[40]), which is caused by the presence of $Li_2Br_2(TMEDA)_2$. In the cocrystallized $Li_2Br_2(TMEDA)_2$ each lithium atom is coordinated by two bridging bromine atoms and two nitrogen atoms (Figure 4b).

Attempts to perform the methylation reaction of complex **3** with (TMEDA)$MgMe_2$ in an ether solution at low temperature instead of with MeLi produced the fully reduced complex (TMEDA)$_2$Ni(0) (**7**) (eq 5).

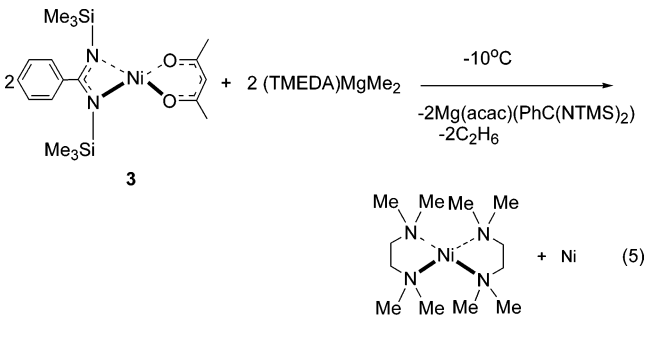

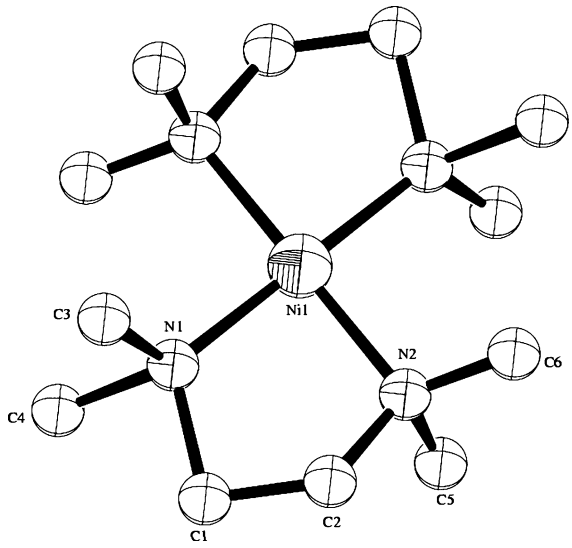

Figure 5. ORTEP diagram of complex **7**. Thermal ellipsoids are given at the 50% probability level.

Complex **7** has a symmetrical square-planar geometry, and the low-temperature X-ray crystal structure is presented in Figure 5. Crystallographic data and structure refinement details for the complex are given in Table 2. The four Ni−N bond lengths of the two chelate units are equidistant (Ni(1)−N(2) = 1.991(13) Å, Ni(1)−N(1) = 2.010(11) Å), and its square-planar symmetry is corroborated by the sum of the angles around the nickel center (360.00°) (N(2)−Ni(1)−N(1)#1 = 94.1(6)°, N(2)−Ni(1)−N(1) = 85.9(6)°) and the transoid angle N(2)−Ni(1)−N(2)#1 = 179.999(1)°.

Synthesis of the Complexes (*N*,*N*′-Bis(trimethylsilyl)-*p*-toluimidinate)(acetylacetonate)nickel (8), (*N*,*N*′-bis(trimethylsilyl)-*p*-toluimidinate)(acetylacetonate)(tetramethylethylenediamine)nickel (9), and Bis(μ$_2$-*N*,*N*′-bis(trimethylsilyl)-*p*-toluimidinate)nickel (10). To study electronic effects on the reactivity we have performed the reaction between the ligand **1b**, containing a *p*-methyl substituent in the aromatic ring, and an equimolar amount of complex **2** in toluene at ambient temperature. The reaction produces a mixture of three compounds, which can be separated in low yields by continuous fractional crystallizations: *p*-MePhC(NSiMe$_3$)$_2$Ni(acac) (**8**), *p*-MePhC(NSiMe$_3$)$_2$Ni(acac)(TMEDA) (**9**), and [*p*-MePhC(NSiMe$_3$)$_2$]$_2$Ni (**10**) (eq 6).

The solid-state molecular structures of complexes **8**−**10** were confirmed by single-crystal X-ray diffraction studies. ORTEP diagrams are presented in Figures 6−8, respectively, whereas crystallographic data and structure refinement details for the complexes are collected in Tables 2 and 3. Selected bond lengths and angles are collected in Tables 4 and 5. The X-ray analysis of the bright red complex **8** shows that the nickel atom adopts a slightly distorted square planar geometry chelated by one acetylacetonate ligand and one slightly puckered *p*-toluimidinate ligand (N(1)−Ni−N(2)−C(4) = 1.2°). Interestingly, in the comparison of complex **8** with the aforementioned complex **3**, there are no significant differences observed for the first coordination sphere around the nickel center and Ni−N and Ni−O bond

(40) Walther, D.; Gebhardt, P.; Fischler, R.; Kreher, U.; Gorls, H. *Inorg. Chim. Acta*, **1998**, *281*, 181.

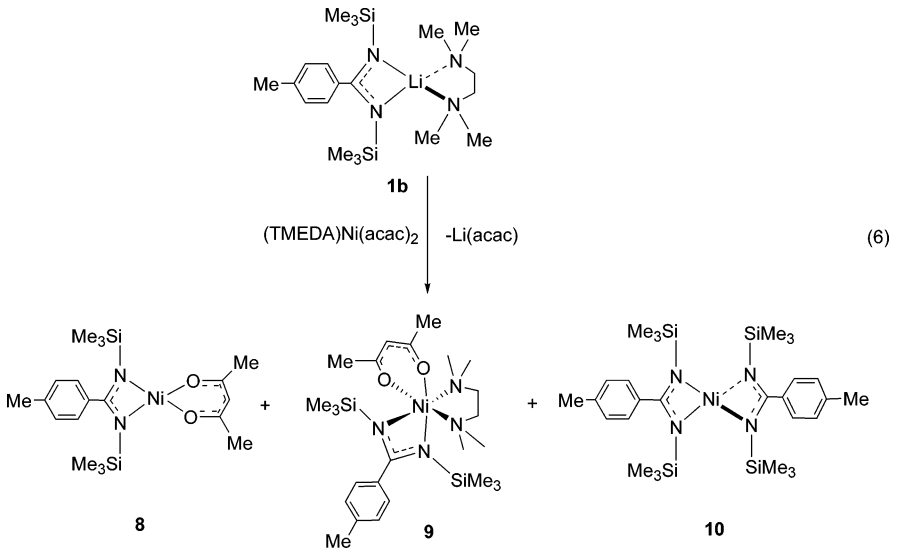

lengths and bond angles. This indicates that the existence of an electron-donating *p*-methyl group in the benzamidinate ligation does not exert a noticeable impact on the coordination structure.

The crystal structure of the green complex **9** reveals that the central nickel atom is connected similarly to complex **4** with one *p*-toluimidinate ligand, one acetylacetonate ligand, and one TMEDA molecule disposed in a distorted-octahedral environment. The oxygen atom O(1) and the N(1), N(3), and N(4) nitrogen atoms lie in the equatorial positions, whereas the nitrogen atom N(2) and oxygen atom O(2) occupy the distorted axial coordination sites.

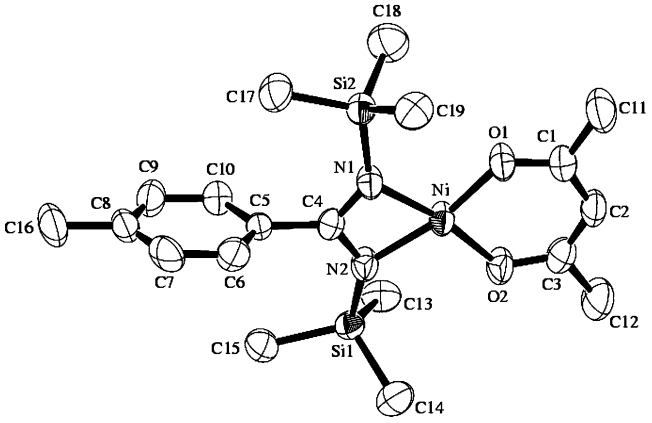

Figure 6. ORTEP diagram of complex **8**. Thermal ellipsoids are given at the 50% probability level.

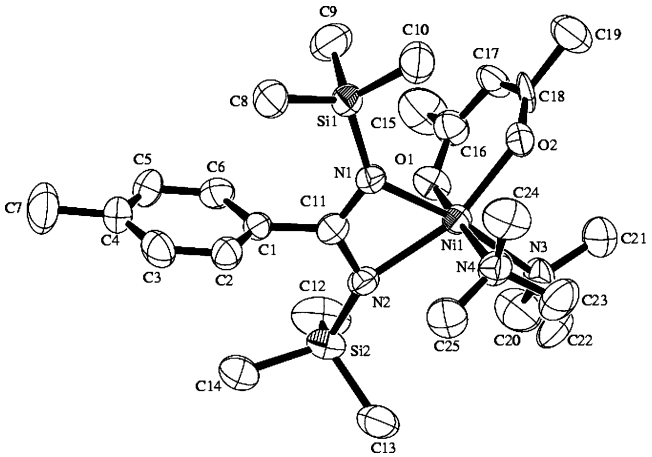

Figure 7. ORTEP diagram of complex **9**. Thermal ellipsoids are given at the 50% probability level.

Similar to the relationship between complexes **8** and **3**, the addition of the methyl substituent in complex **9** did not cause much difference as compared to complex **4**. In a comparison of the reactions (eqs 1 and 6), it is clear that the main effect of the *p*-methyl substituent at the aromatic ring is the formation of the bis(bis(trimethylsilyl)toluimidinate)nickel complex **10** that is similar to complex **6**, which was obtained either via a disproportionation pathway (eq 3) or via a reaction with different starting materials (eq 4).

The X-ray solid-state structure of complex **10** indicates that the nickel is chelated by two *p*-toluimidinate ligands in a distorted-tetrahedral geometry. The two four-membered Ni−N−C−N rings are symmetrical with both Ni−N and C(ipso)−N bond lengths being alike (Ni(1)−N(2) = 1.990(3) Å, Ni(1)−N(1)#1 = 2.019(3) Å, N(1)−C(13) = 1.327(5) Å, N(2)−C(11) = 1.323(5) Å). The Ni−N bond lengths in complex **10** are almost equidistant and similar to those in the reported bis(benzamidinate)nickel complex and in complex **6**. When the geometrical characteristics of the benzamidinate ligands for complexes **10** and **6** and for the reported Ni(II) complex are compared, interesting features can be observed. The dissimilarity of the N−Ni−N angles (see Table 5) and the differences in the bending along the central ipso carbons are as follows: C(11)−Ni−C(11)#1 = 152.8(2)°

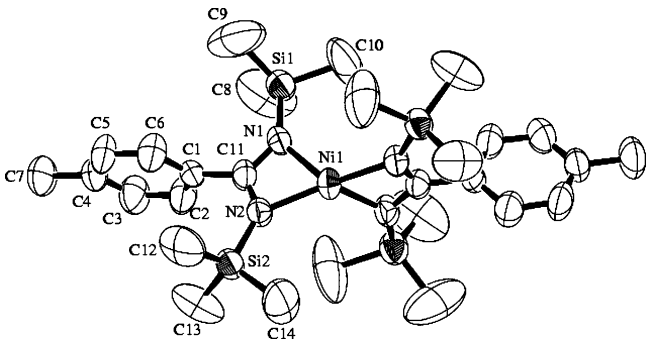

Figure 8. ORTEP diagram of complex **10**. Thermal ellipsoids are given at the 50% probability level.

for complex **10**, C(6)−Ni−C(23) = 159.3(3)° for complex **6**, and C(6)−Ni−C(23) = 159.4(2)° for the reported Ni(II) compound.[40] The comparison indicates that the existence of a *p*-methyl group in the benzamidinate ligand affects the arrangement of the first coordination ligand sphere around the nickel center in complex **10**.

Synthesis of Bis(pyridine)dimethylnickel(II) (11). In our attempts to prepare a stable nickel complex containing a methyl group that can be activated for catalytic purposes, we decided to prepare bis(pyridine)-dimethylnickel(II) (**11**). This complex was obtained by the reaction of (TMEDA)$NiMe_2$, synthesized via a procedure described in the literature,[10d,32a] with a 10-fold excess of pyridine at low temperature (eq 7).

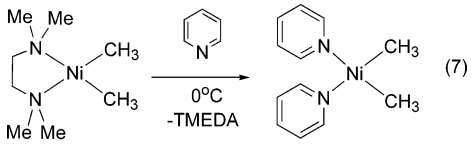

(7)

11

Interestingly, a similar pyridine-substituted complex was prepared from the reaction of $NiCl_2Py_4$ with CH_3-MgX or MeLi,[41] although its stability was found to be low and its crystal structure was not determined.

Complex **11** was successfully crystallized from a toluene solution to obtain red-brown single crystals suitable for X-ray measurements. Complex **11** has a nearly ideal square-planar geometry, and the low-temperature X-ray crystal structure is presented in Figure 9. Crystallographic data and structure refine-

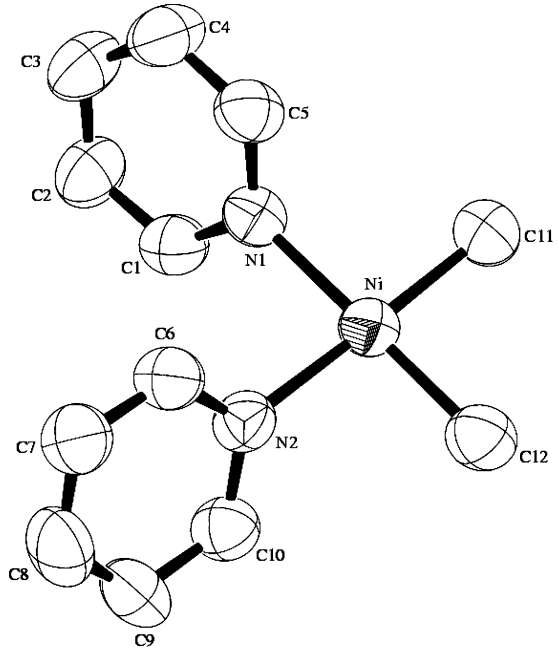

Figure 9. ORTEP diagram of complex **11**. Thermal ellipsoids are given at the 50% probability level.

ment details for the complex are given in Table 3. The nickel is surrounded by two pyridine molecules and two methyl groups (C(11)−Ni−C(12) = 89.5(2)°, C(11)−Ni−N(1) = 90.4(2)°). The pyridine ring is disposed with a dihedral angle of 132.86° with regard to the nickel−dimethyl plane. Complex **11** was found to be also not very stable and decomposes, yielding black Ni(0) in solution with $t_{1/2}$ = 45−60 min at room temperature. As a solid, the complex is rather stable for a few weeks at room temperature.

Selected bond lengths (Å) and angles (deg) for complex **11**: Ni−C(11) = 1.908(5), Ni−C(12) = 1.918(5), Ni−N(1) = 1.961(4), Ni−N(2) = 1.976(4); C(11)−Ni−C(12) = 89.5(2), C(11)−Ni−N(1) = 90.4(2), C(12)−Ni−N(1) = 178.4(2), C(11)−Ni−N(2) = 178.3(2), C(12)−Ni−N(2) = 92.2(2), N(1)−Ni−N(2) = 87.99(2)°.

Synthesis of Bis(μ_2-*N*,*N*′-bis(trimethylsilyl)-*p*-toluimidinate)(pyridine)nickel(II) (14). As described above, the use of a benzamidinate or toluimidinate lithium ligand induces the formation of a mixture of compounds. In a different strategy to try to obtain an alkylnickel complex, we have performed the protonolysis of the lithium *p*-toluimidinate compound **1b** with Et_3-NHCl in toluene at ambient temperature to yield the neutral *p*-MePhC($NSiMe_3$)($NHSiMe_3$) (**12**) in 81% yield (eq 8).

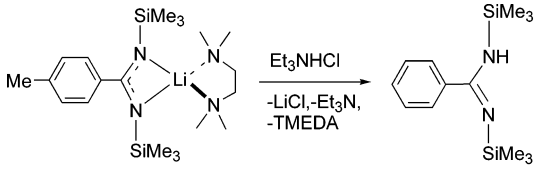

(8)

1b **12**

The reaction of (TMEDA)$NiMe_2$ with the neutral ligand **12** in a solution mixture of toluene and pyridine (3:1) initially provided the expected methyl complex **13**, which could be observed on following the crude reaction by ^{1}H NMR (δ −0.25, corresponding to Ni−CH_3). The signal disappears as a function of time, and the repeated washing of the precipitated complex with cold toluene

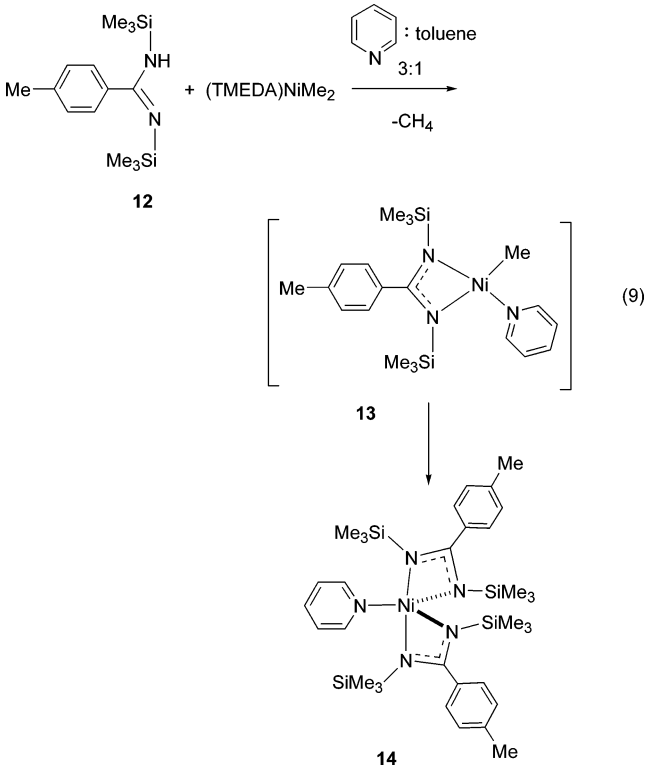

(9)

12 **13** **14**

(41) Campora, J.; Conejo, M.; Mereiter, K.; Palma, P.; Perez, C.; Reyes, M. L.; Ruiz, C. *J. Organomet. Chem.* **2003**, *683*, 220.

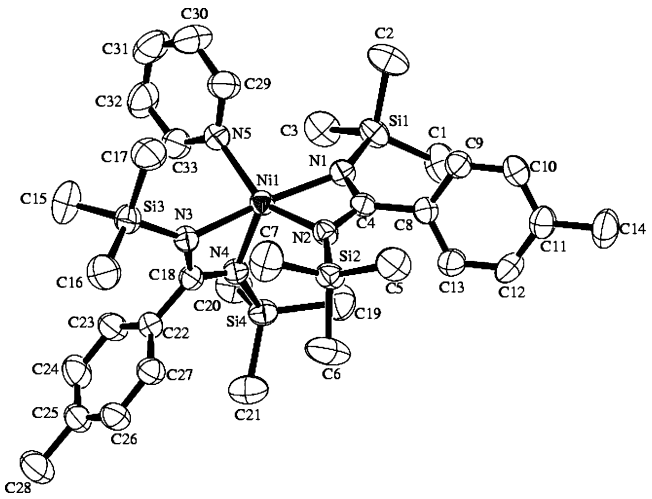

Figure 10. ORTEP diagram of complex **14**. Thermal ellipsoids are given at the 50% probability level.

and recrystallization at −30 °C for 2 weeks afforded green single crystals of complex **14** (eq 9).

The molecular structure of **14** was confirmed by low-temperature X-ray crystallography. Crystallographic data and structure refinement details for the complex and selected bond lengths and angles are given in Tables 3 and 5, respectively. Figure 10 reveals that the geometry of the nickel center is a distorted-trigonal bipyramid with N(1) and N(3) at the axial positions having the longer bond lengths to the metal (Ni(1)−N(1) = 2.083(2) Å, Ni(1)−N(3) = 2.104(2) Å) as compared to the lengths for the other three nitrogen atoms forming the equatorial plane. (The sum of the equatorial angles is 359.45°; N(2)−Ni(1)−N(5) = 151.16(9)°, N(4)−Ni(1)−N(5) = 102.76(9)°, N(4)−Ni(1)−N(2) = 105.53(9)°.)

The two four-membered Ni−N−C−N rings are almost symmetrical with both Ni−N and C(ipso)−N bond lengths being alike (Ni(1)−N(4) = 2.050(2) Å, Ni(1)−N(2) = 2.063(2) Å, N(1)−C(4) = 1.330(3) Å, N(2)−C(4) = 1.321(3) Å, N(3)−C(18) = 1.333(3) Å, N(4)−C(18) = 1.328(3) Å). The angles N(2)−Ni(1)−N(1) = 65.59(9)° and N(4)−Ni(1)−N(3) = 65.56(9)° are similar to those exhibited by complexes **4** (63.56(7)°), **9** (63.96(16)°), **10** (67.65(13)°), and **6** (68.7(2)°), while somewhat smaller than those exhibited in the square-planar complexes **3** (69.74(10)°) and **8** (70.02(8)°).

Interestingly, the pyridine distance to the metal center is greater (Ni−N(5) = 2.076(2) Å) as compared to the pyridine−metal distance exhibited in complex **11** (1.976(4) Å), due to the steric hindrance imposed by the two *p*-toluimidinate ligands and the difference in the coordination numbers.

Catalytic Studies of Complex 3 Activated by MAO. (a) Polymerization of Norbornene. Complex **3** has been studied as a catalytic precursor for the polymerization of norbornene. Control experiments were performed to identify the possible catalytic activity of each one of the single components. Complex **3** was found to be not an active catalyst for the polymerization of norbornene in the absence of MAO in any of the studied solvents (toluene and dichloromethane). Also, no polymer formation was observed when MAO alone was used in toluene. However, when MAO was used either with dichloromethane or with hexane, it was found that MAO is able to activate norbornene toward polynorbornenes, giving 35% or 18% yield, respectively, over a period of 5 h. The NMR structures of the polymers obtained with MAO in dichloromethane and hexane are totally different, which is plausible because they are obtained through a simple cationic mechanism. Thus, all the polymerization studies were carried out in toluene. The use of MAO as a cocatalyst leads to the formation of aluminum salts that are absorbed into the polymer upon quenching the reaction, and their full removal was found to be rather difficult. Therefore, we decided to minimize the MAO to precatalyst ratio while maintaining the maximum catalytic activity. The activity of the catalyst and the molecular weights of the resulting polynorbornenes are affected by reaction conditions such as reaction time, MAO to precatalyst ratio, and reaction temperature. The polymerization results are presented in Table 6, showing that complex **3** activated with MAO is an excellent catalyst for the polymerization of norbornene in toluene. Two different catalyst activation processes were tested. In the first procedure, the precatalyst and MAO were mixed, generating the active sites before the addition of norbornene. The second procedure was based on the activation of complex **3** with MAO in the presence of the monomer. Table 6 shows that the first procedure gave higher catalytic activities (compare entries 1 and 6, 2 and 12, or 3 and 7).

Table 6. Data for the Polymerization of Norbornene Promoted by the 3/MAO System[a]

entry	Al:Ni	*T*, °C	time, h	yield, %	activity × 10^{-3} [c]	$M_w \times 10^{-3}$	M_w/M_n
1[b]	100	25	0.25	47	180	378	2.5
2[b]	100	25	1	57	54	328	2.6
3[b]	200	25	0.25	56	210	324	2.6
4	25	25	0.25	13	49	377	2.4
5	50	25	0.25	27	100	406	2.1
6	100	25	0.25	52	200	408	2.3
7	200	25	0.25	59	220	331	2.5
8	400	25	0.25	63	240	252	2.5
9	700	25	0.25	70	260	210	2.3
10	1000	25	0.25	67	250	232	2.6
11	100	25	0.5	59	110	433	2.0
12	100	25	1	66	62	354	1.9
13	100	25	2	80	38	356	2.8
14	100	25	6	84	13	359	2.0
15	100	0	0.25	81	310	356	3.3
16	100	25	0.25	52	200	408	2.3
17	100	40	0.25	38	150	219	2.3
18	100	70	0.25	41	150	201	2.7

[a] Reaction conditions: [Ni] = 1.06×10^{-3} M; [monomer]:[Ni] = 1000; 5 mL of toluene. [b] The activation of complex **3** with MAO in the presence of monomer. [c] In units of g of PNB (mol of Ni)$^{-1}$ h^{-1}.

Starting at a low MAO amount, up to a molar ratio of Al:Ni = 500, the polymer yields and the catalyst activity rise with an increase in the MAO concentration (compare entries 4−10). Interestingly, the reaction profile is very similar to those obtained for (salicylaldiminato)nickel[42] and $Ni(acac)_2$[21b] complexes being activated with MAO (for (salicylaldiminato)nickel, 38% yield at Al:Ni = 500, [monomer]:[Ni] = 5000, t = 0.5 h; for $Ni(acac)_2$, 40% yield at Al:Ni = 100, [monomer]:[Ni] = 1500, t = 4 h).

The molecular weights of the polymers as a function of the MAO amount were found to increase up to a maximum where the Al:Ni ratio is ∼100 (Figure 11;

(42) Sun, W.-H.; Yang, H.; Li, Z.; Li, Y. *Organometallics* **2003**, *22*, 3678.

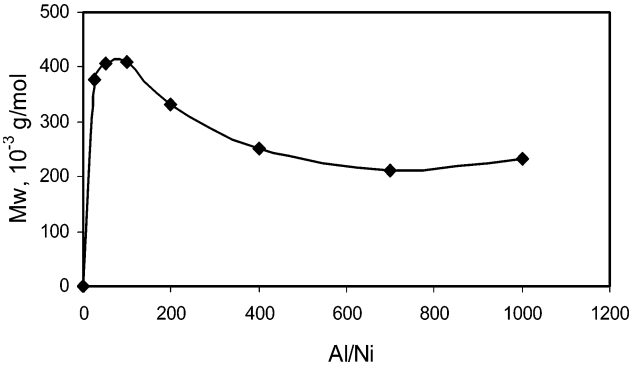

Figure 11. Dependence of the weight-average molecular weight on the MAO to precatalyst ratio. Reaction conditions: [Ni] = 1.06×10^{-3} M; [monomer]:[Ni] = 1000; 0.25 h, 25 °C.

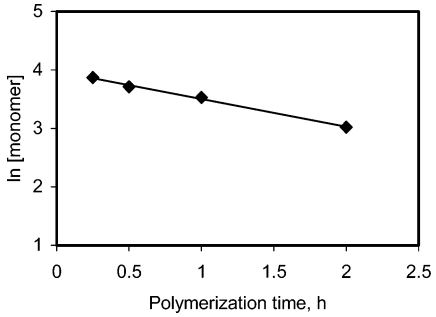

Figure 12. First-order dependence of the monomer in the polymerization of norbornene. Reaction conditions: [Ni] = 1.06×10^{-3} M; [monomer]:[Ni] = 1000; Al:Ni = 100; 25 °C.

Table 6, entries 5 and 6). Higher MAO to precatalyst ratios result in the lowering of the M_w value of the polymer, reaching a plateau around $M_w \approx 200\,000$. Therefore, all the following studies were performed at an MAO to precatalyst ratio of 100.

As shown in Table 6, the polymerization time considerably affects the polymer yields, the molecular weights of the polymers, and the catalytic activities (see entries 6 and 11−14). The polymer yield sharply increases in the initial 0.5 h period, reaching a value of 59% (as a comparison, for $Ni(acac)_2$ 70% yield is obtained at Al:Ni = 1000 over 0.5 h). Longer reaction times lead to a modest increase in the yields (84% for 6 h) (for $Ni(acac)_2$ 72% yield polynorbornene is produced at Al:Ni = 1000 over 5 h).[21b]

Interestingly, the formation of polynorbornene with catalyst **3** follows a first-order dependence in monomer, yielding $k = 3.04 \times 10^{-4}$ s^{-1}, as presented in Figure 12. Since the activation of the precatalysts by the MAO cocatalyst is a fast process and the chain termination reaction must be the rate-determining step in the polymerization reaction, the first-order dependence in monomer indicates that the chain to olefin transfer pathway is plausible as the main operative chain termination mechanism. This result is corroborated by the kinetic competition observed when the polymerization is conducted with large concentrations of MAO, inducing a reduction in the polymer molecular weights.

It is noteworthy that the consecutive introduction of a new portion of the monomer after 0.25 h results in a considerable increase in the yield of polynorbornene after a subsequent reaction time of 0.25 h, keeping the

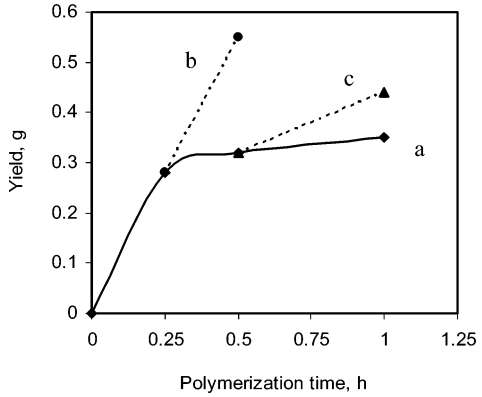

Figure 13. Follow-up in the polymerization of norbornene after subsequent introduction of a new portion of the monomer after 0.25 h (b) and 0.5 h (c) and without addition of the monomer (a). Reaction conditions: [Ni] = 1.06×10^{-3} M; Al:Ni = 100, 25 °C.

reaction rate at a constant level (Figure 13, compare plots a and b). Addition of a new portion of the monomer after 0.5 h also increases the yield of polynorbornenes, but to a lesser extent, decreasing the reaction rate (Figure 13, compare plots a and c). This result indicates that the diffusion of the monomer through the formed polymer to the active centers at a longer reaction time may become the rate-determining stage. The formation of the polymer as a function of time reveals that polynorbornene starts to precipitate after 0.5 h, trapping both monomer and catalyst. Therefore, if the addition of new portions of the monomer is performed before the precipitation, a linear rate correlation can be maintained.

When the reaction temperature is reduced from 70 to 0 °C, keeping Al:Ni = 100 and a norbornene to precatalyst ratio of 1000, this results in an augmentation of the polymer yield while a maximum crest is again observed at 25 °C in the molecular weights of the produced polynorbornenes (Table 6, entries 6 and 15−18). This result indicates that higher temperatures induce some deactivation of the active sites in addition to more effective termination pathways.

Analogous effects of the temperature on the polymer yield and the activity have been shown for a bis(1-aryliminomethylnaphthalen-2-oxy)nickel complex (a 2-fold increase in activity was observed by decreasing the reaction temperature from 100 to 0 °C).[43] A similar tendency was also observed for a (salicylideneiminato)-nickel(II) complex.[25] In contrast to complex **3**, an increase in polymer yield and catalytic activity has been observed by increasing the polymerization temperature for (2-methyl-8-(diphenylphosphino)quinoline)nickel,[44] whereas for $Ni(acac)_2$ there is no effect on the polymerization temperature.[21b]

All polymers were characterized by ^{1}H NMR, ^{13}C NMR, and FTIR spectroscopy, indicating the absence of carbon−carbon double bonds that is typical for ROMP polynorbornenes.[45] In addition, no ^{1}H NMR resonances are observed for vinylic hydrogens between 5 and 6.7

(43) Chang, F.; Zhang, D.; Xu, G.; Yang, H.; Li, J.; Song, H.; Sun, W.-H. *J. Organomet. Chem.* **2004**, *689*, 936.
(44) Yang, H.; Li, Z.; Sun, W.-H. *J. Mol. Catal. A: Chem.* **2003**, *206*, 23.
(45) Haselwander, T. F. A.; Heitz, W. *Macromol. Rapid Commun.* **1997**, *18*, 689.

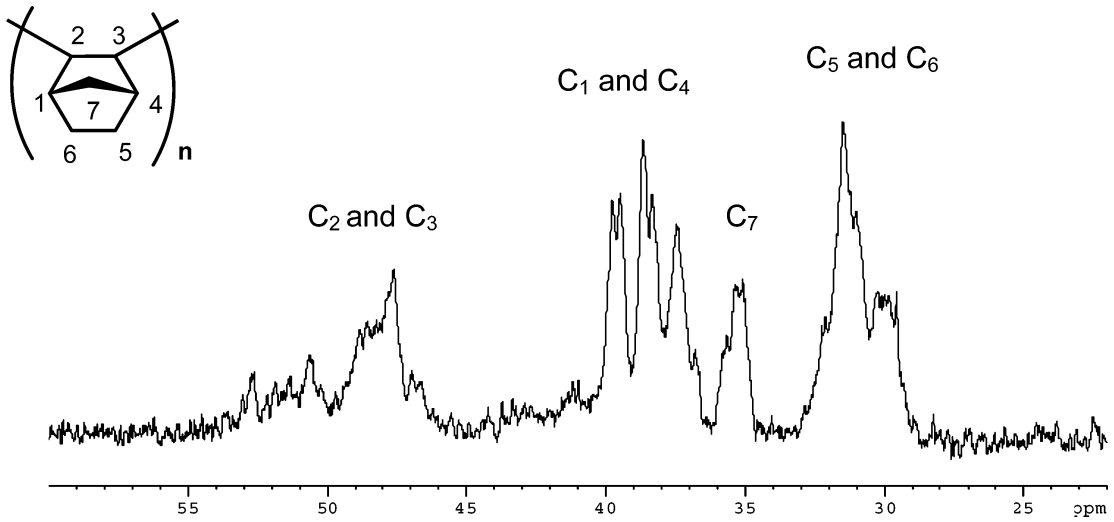

Figure 14. ^{13}C NMR of polynorbornene produced by complex **3** with MAO in toluene.

ppm, and no absorptions were observed between 1620 and 1680 cm^{-1} in the IR spectra. The ^{13}C NMR spectra of polynorbornenes synthesized with **3**/MAO catalytic system present four groups of resonance at 29−32 ppm for C_5 and C_6, 35−36 ppm for C_7, 37−40 ppm for C_1 and C_4, and 47−52 ppm for C_2 and C_3. The ^{13}C NMR spectra are similar to those reported for $Ni(acac)_2$,[21b] pyrrolimine,[23] and bis(benzimidazole)nickel catalyst,[46] indicating that the obtained polynorbornenes using the catalytic system **3**/MAO are vinyl-type addition polymers (Figure 14).

(b) Dimerization of Propylene. The reaction of complex **3** with propylene and MAO (MAO to precatalyst ratio of 200) generates various dimerization products with a remarkable turnover frequency of 9040 h^{-1}. The reaction has been performed at liquid propylene (10 bar) and at room temperature without additional solvents (eq 10).

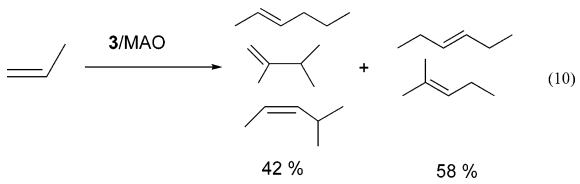

(10)

This complex shows a large selectivity toward dimers (>98%), as determined by GC and GC-MS. Two mixtures of hexenes containing both primary dimerization products (42%, *trans*-2-hexene, 2,3-dimethyl-1-butene, *cis*-4-methyl-2-pentene) and isomerization products (58%, *trans*-3-hexene, 2-methyl-2-pentene) were obtained. No trimers, tetramers, or higher oligomers were detected over a reaction period of 1 h; however, trace amounts of trimers appear only at longer reaction periods. Interestingly, a similar selectivity with a different product distribution was observed for α-diimine nickel complexes.[47]

(c) Oligomerization of Ethylene. Complex **3** was also tested as a precatalyst for the oligomerization of ethylene when activated with MAO (Al:Ni = 200). Performing the reaction in toluene, at ambient temperature and a constant ethylene pressure of 30 atm, affords the extremely rapid production of a mixture of dimers (52%) and trimers (48%) with a turnover frequency of 17 050 h^{-1} (Table 7).

Table 7. Data for the Oligomerization of Ethylene Promoted by Complex 3 Activated by MAO[a]

		amt, %					
solvent	*T*, C	C_4H_8	C_6H_{12}	C_8-C_{12}[b]	C_8-C_{14}	Schulz−Flory α	TOF[c] (η), h^{-1}
toluene	25	52	48			0.48	17 100
CH_2Cl_2	25	28	44	28		0.72	43 600
CH_2Cl_2	70	17	39		44	0.83	83 500

[a] Reaction conditions: [Ni] = 1.2×10^{-3} M, Al:Ni = 200, time 1 h, solvent 10 mL, 30 bar of ethylene. [b] C_8-C_{12} = hydrocarbons with 8−12 carbons in the chain. [c] TOF = turnover frequency (in units of (mol of ethylene) (mol of catalyst)$^{-1}$ h^{-1}).

The product distribution and the catalyst selectivity in toluene have been found to be unaffected by the reaction time (from 1 to 2 h). Interestingly, using dichloromethane as a solvent under the same reaction conditions leads to oligomers of ethylene in the C_4-C_{12} range, which are distributed as 28% butenes, 44% hexenes, and 28% of the mixture C_8-C_{12} (Table 7). The oligomerization follows a Schulz−Flory distribution[48] that is characterized by the constant α. This constant represents the probability for chain propagation as displayed in eq 11. An oligomer distribution with a small

$$\alpha = \frac{\text{rate of propagation}}{\text{rate of propagation} + \text{rate of chain transfer}} = \frac{\text{moles of } C_{n+2}}{\text{moles of } C_n} \quad (11)$$

α value (e. g. α < 0.5) is indicative of mainly dimers and lower oligomers. A high value indicates higher oligomers. As presented, mainly dimers are the oligomers obtained.

Performing the oligomerization reaction at a temperature of 70 °C for 1 h leads to oligomers of ethylene in the C_4-C_{14} range having a different product distribution, with a larger amount of the higher oligomers (17%

(46) Patil, A. O.; Zushma, S.; Stibrany, R. T.; Rucker, S. P.; Wheeler, L. M. *J. Polym. Sci. A: Polym. Chem.* **2003**, *41*, 2095.
(47) Svejda, S. A.; Brookhart, M. *Organometallics* **1999**, *18*, 65.
(48) (a) Flory, P. J. *J. Am. Chem. Soc.* **1940**, *62,* 1561. (b) Schulz, G. V. *Z. Phys. Chem., Abt. B* **1935**, *30*, 379. (c) Schulz, G. V. *Z. Phys. Chem., Abt. B* **1939**, *43*, 25.

of butenes, 39% of hexenes, and 44% of C_8-C_{14}) (Table 7). Interestingly, in the oligomerization of ethylene under all the reaction conditions, all the products were linear. No branched propenes, butenes, or pentenes were observed. In addition, among the linear olefins, the ratio of α-olefins to internal olefins is almost not affected by the solvent (20:80, respectively). However, when the reaction is carried out at higher temperatures (70 °C), the terminal to internal alkene ratio changes to 12:88, respectively, as expected due to the thermodynamic stability of the more substituted alkenes.

Conclusions

Seven new nickel complexes bearing the chelating benzamidinate ligand have been synthesized. Their solid-state molecular structures have been determined by low-temperature X-ray diffraction analysis. In addition, the solid-state structure of dimethylbis(pyridine)-nickel was obtained. Complex **3** activated with MAO has been shown to be an efficient catalytic system for the norbornene vinyl-type polymerization. In addition, this catalytic system has been found to dimerize propylene to a mixture of hexenes and oligomerize ethylene to either C_4-C_6 or C_4-C_{14} products, depending on the temperature and the solvent used in the reaction.

Acknowledgment. This research was supported by the German Israel Foundation under Contract I-621-27.5/1999 and by the Fund for the Promotion of Research at the Technion.

Supporting Information Available: Tables giving crystallographic data for complexes **3**−**11** and **14**; these data are also available as CIF files. This material is available free of charge via the Internet at http://pubs.acs.org.

OM0490379